ACS central science

Outlook

Cite This: ACS Cent. Sci. 2019, 5, 13−28

http://pubs.acs.org/journal/acscii

Heme and Nonheme High-Valent Iron and Manganese Oxo Cores in Biological and Abiological Oxidation Reactions

Mian Guo,[†,#] Teresa Corona,[‡,#] Kallol Ray,*[,‡] and Wonwoo Nam*[,†,§]

[†]Department of Chemistry and Nano Science, Ewha Womans University, Seoul 03760, Korea

[‡]Department of Chemistry, Humboldt-Universität zu Berlin, Brook-Taylor-Strasse 2, 12489 Berlin, Germany

[§]State Key Laboratory for Oxo Synthesis and Selective Oxidation, Center for Excellence in Molecular Synthesis, Suzhou Research Institute of LICP, Lanzhou Institute of Chemical Physics (LICP), Chinese Academy of Sciences, Lanzhou, 730000, P. R. China

ABSTRACT: Utilization of O_2 as an abundant and environmentally benign oxidant is of great interest in the design of bioinspired synthetic catalytic oxidation systems. Metalloenzymes activate O_2 by employing earth-abundant metals and exhibit diverse reactivities in oxidation reactions, including epoxidation of olefins, functionalization of alkane C−H bonds, arene hydroxylation, and *syn*-dihydroxylation of arenes. Metal−oxo species are proposed as reactive intermediates in these reactions. A number of biomimetic metal−oxo complexes have been synthesized in recent years by activating O_2 or using artificial oxidants at iron and manganese centers supported on heme or nonheme-type ligand environments. Detailed reactivity studies together with spectroscopy and theory have helped us understand how the reactivities of these metal−oxygen intermediates are controlled by the electronic and steric properties of the metal centers. These studies have provided important insights into biological reactions, which have contributed to the design of biologically inspired oxidation catalysts containing earth-abundant metals like iron and manganese. In this Outlook article, we survey a few examples of these advances with particular emphasis in each case on the interplay of catalyst design and our understanding of metalloenzyme structure and function.

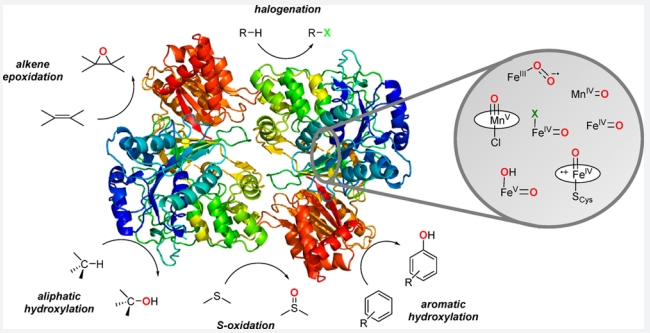

1. INTRODUCTION

Dioxygen (O_2) is kinetically quite stable toward reaction at room temperature because of its triplet ground state, which makes its two-electron reaction with closed shell reaction partners like typical organic compounds spin-forbidden.[1−4] The single electron reduction of triplet oxygen ($^3O_2$) to the superoxide anion is also unfavorable by 7.8 kcal mol^{-1}.[5] Nevertheless, the overall four-electron reductive activation of O_2 is thermodynamically favorable with a redox potential of 0.815 V vs NHE in water at pH 7 and 25 °C.[5] Nature is able to harness the strong oxidizing capability of O_2 by overcoming the spin state barrier by activating $^3O_2$ at transition metal ions, which also possess open-shell spin ground states.[6,7] These metal ions help to initiate the one-electron reduction of O_2 by metal coordination and also act as multielectron reductants to access thermodynamically more favorable two-electron or even four-electron reduction pathways.[8−11] First-row transition metal ions, such as Fe and Cu, are often employed by metalloenzymes for the reductive activation of O_2 to carry out a variety of important biological processes.[1−3,6,7]

The ability of iron to access multiple redox states, as well as its bioavailability, makes it one of the most common transition metals used for biological O_2-activation.[1−3,12−14] Further, there are a number of open-shell spin states available in the different common oxidation states of iron, with high-spin Fe(II) being the most relevant with regard to the binding and activation of O_2. The heme-containing peroxidases, oxygenases, and catalases comprise mononuclear iron protoporphyrin IX active sites coordinated to either a cysteine, tyrosine, or histidine residue, respectively (Figure 1A; Heme).[15] In nonheme iron enzymes, in contrast, a common structural motif utilized for dioxygen activation is the facial orientation of iron with two histidine ligands and one carboxylate ligand, namely, a 2-His/1-Asp (or 1-Glu) ligand environment (Figure 1A; Nonheme, Rieske Dioxygenase).[16−19] A 3-His ligand coordination environment has also been observed in a few cases, such as in a number of sulfur-activating nonheme iron dioxygenases (Figure 1A; nonheme, CDO).[16−19] Very often enzymatic activation of dioxygen occurs in the Fe(II) state, leading to a variety of two-electron oxidation processes; a cosubstrate then provides the remaining two electrons necessary for the four-electron reduction of dioxygen (Figure 1B).[16−19] In many cases, 2-oxoacids or tetrahydrobiopterin are used as cosubstrates that deliver two electrons simultaneously to the active site to form peroxoiron(II) and oxoiron(IV) species in the proposed reaction mechanism (Figure 1B; Oxoiron generation).[16−19] Enzymes, such as cytochromes P450 (P450) or

Received: September 30, 2018
Published: December 18, 2018

DOI: 10.1021/acscentsci.8b00698
ACS Cent. Sci. 2019, 5, 13−28

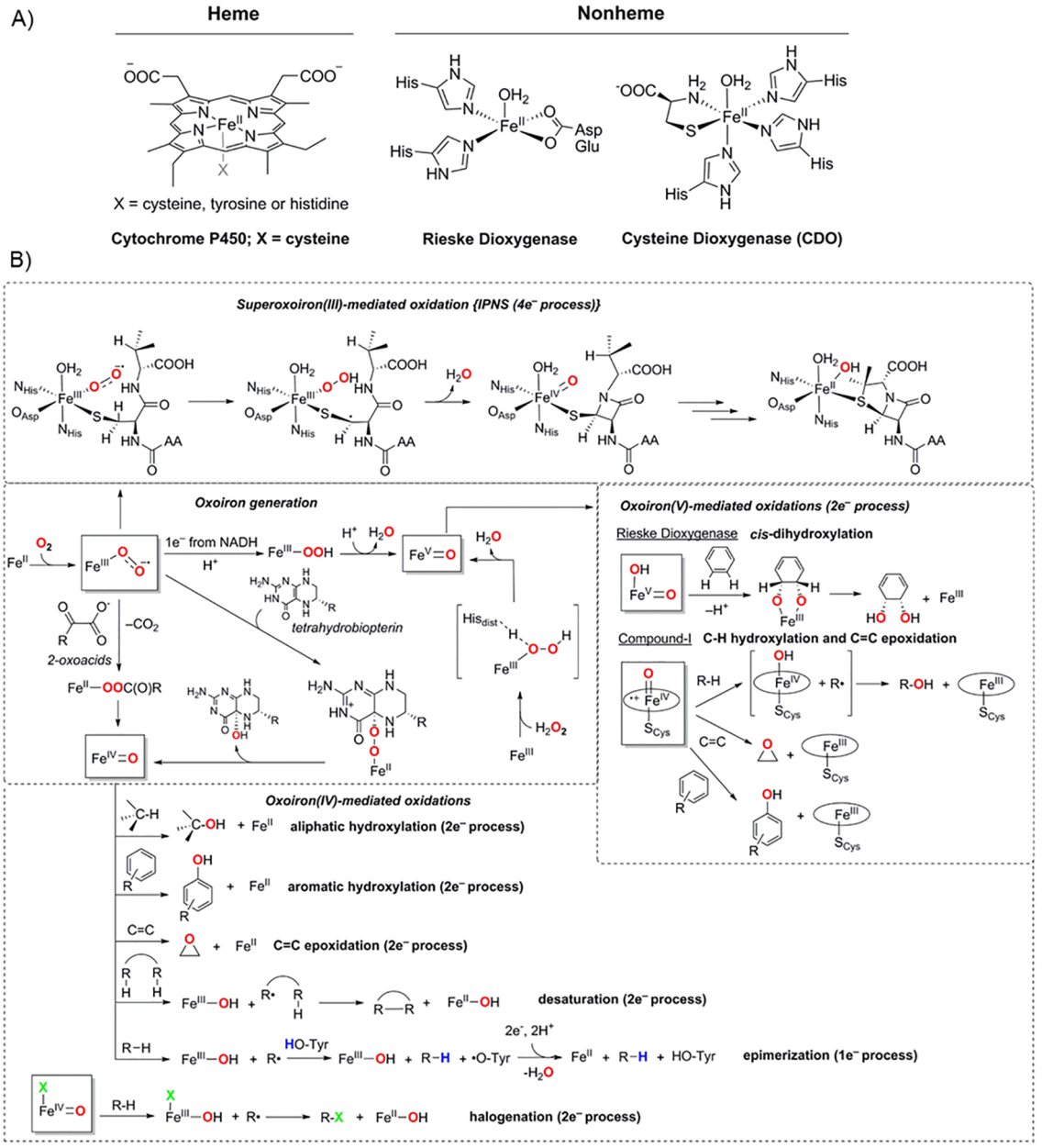

Figure 1. (A) Structures of mononuclear heme and nonheme active sites for dioxygen activation. (B) Mechanisms of dioxygen activation for one-, two-, and four-electron substrate oxidation processes.

Rieske dioxygenases, in contrast, employ NADH as the electron donor to form hydroperoxoiron(III) and formally oxoiron(V) species; all the redox equivalents of the formal oxoiron(V) species are stored either at the metal center as an (OH)Fe^{V}═O intermediate in Rieske dioxygenase or delocalized over the ligand as an oxoiron(IV) porphyrin π-cation radical ion (compound I (Cpd-I) intermediate) in P450.[13,16−19] A second subset of nonheme iron enzymes also initiates four-electron oxidation of substrates by a single equivalent of dioxygen in the absence of any reducing cosubstrates (Figure 1B; isopenicillin-N synthase (IPNS)).[20] This alternative mechanism for iron-mediated dioxygen reduction and C−H activation necessitates an superoxoiron(III) intermediate to initiate catalysis, which may involve a subsequent oxoiron intermediate in the second oxidation step.[18]

The ability of iron to access multiple redox states, as well as its bioavailability, makes it one of the most common transition metals used for biological O_2-activation.

Synthetic biomimetic model complexes have the potential to aid in the understanding of these biological processes. A number of iron model complexes binding oxygen atom(s) have been isolated in recent years;[1,13,18,21−33] detailed reactivity studies together with spectroscopy and theory have helped us understand how the electronic and geometric properties of the iron centers modulate their reactivity. These studies have provided important insights into biological pathways, which

DOI: 10.1021/acscentsci.8b00698
ACS Cent. Sci. 2019, 5, 13−28

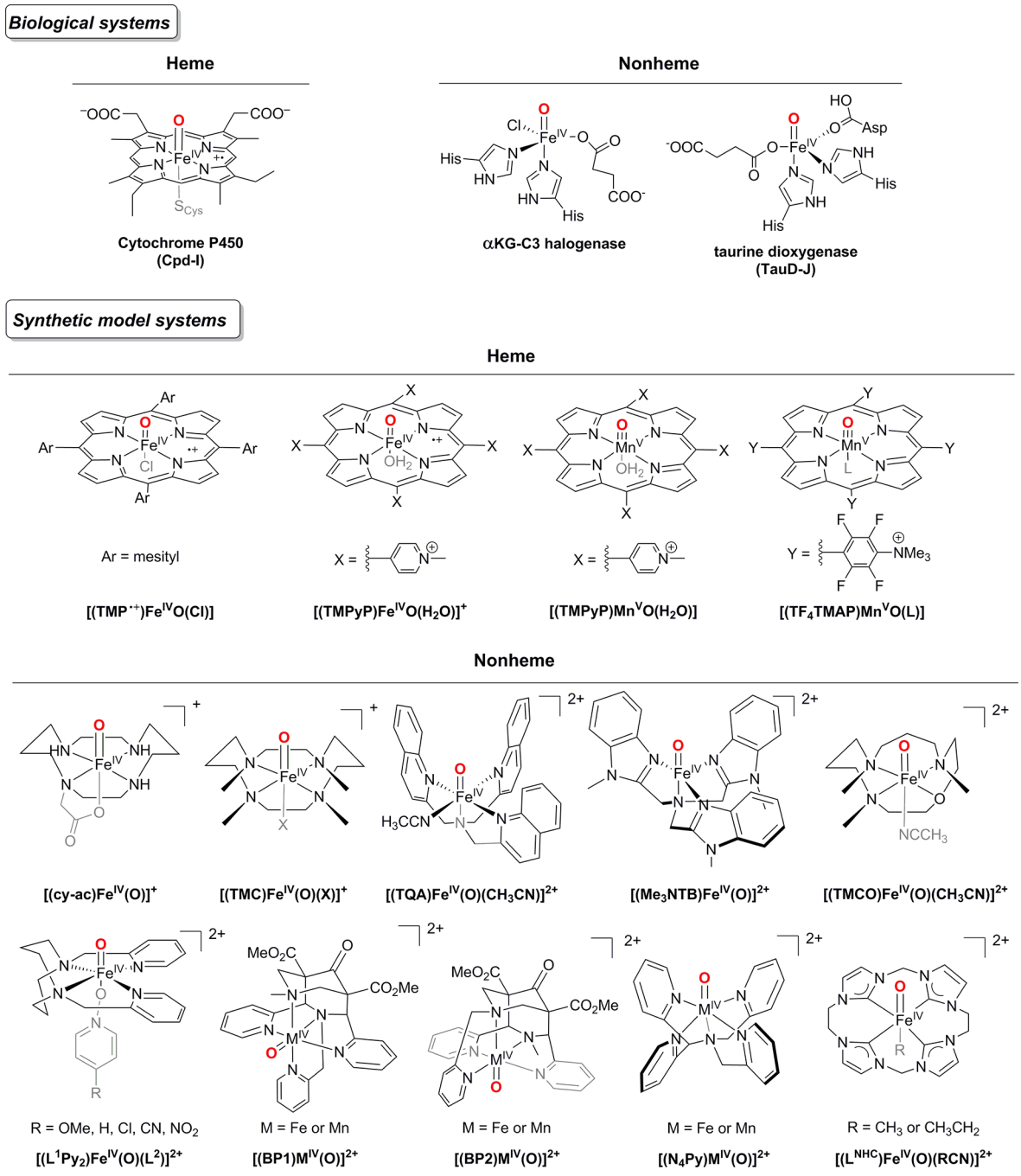

Figure 2. Examples of heme and nonheme intermediates containing oxoiron and oxomanganese cores in biological and synthetic model systems.

have led to a new understanding of the fundamental reaction steps and reactive intermediates relevant to metalloenzymes that incorporate inexpensive and readily available transition metal centers in their active sites, as well as to practical applications. This has eventually contributed to the recent advances in the design of biologically inspired oxidation catalysts containing earth-abundant metals such as iron and manganese.[34−36] In this Outlook article, we survey examples of these advances providing particular emphasis in each case on the interplay of catalyst design and our understanding of metalloenzyme structure and function.

2. HEME SYSTEMS

Biological Intermediates. Cpd-I is the main intermediate responsible for the diverse oxidative reactivities of most heme enzymes.[1,6,7,13,15,37−40] Efforts were mainly dedicated toward the characterization of the Cpd-I intermediate of P450, which proved to be very challenging because of its highly reactive nature. The Cpd-I of other heme-containing enzymes such as horseradish peroxidase (HRP), catalase, and chloroperoxidase (CPO) are much more stable and have been well characterized and unambiguously assigned as an oxoiron(IV) porphyrin π-cation radical species;[15,41−43] however, they did not show any reactivity toward unactivated hydrocarbons. The lack of direct spectroscopic and kinetic characterization of P450 Cpd-I led to the proposition of oxoiron(V) and hydroperoxoiron(III)

DOI: 10.1021/acscentsci.8b00698
ACS Cent. Sci. 2019, 5, 13−28

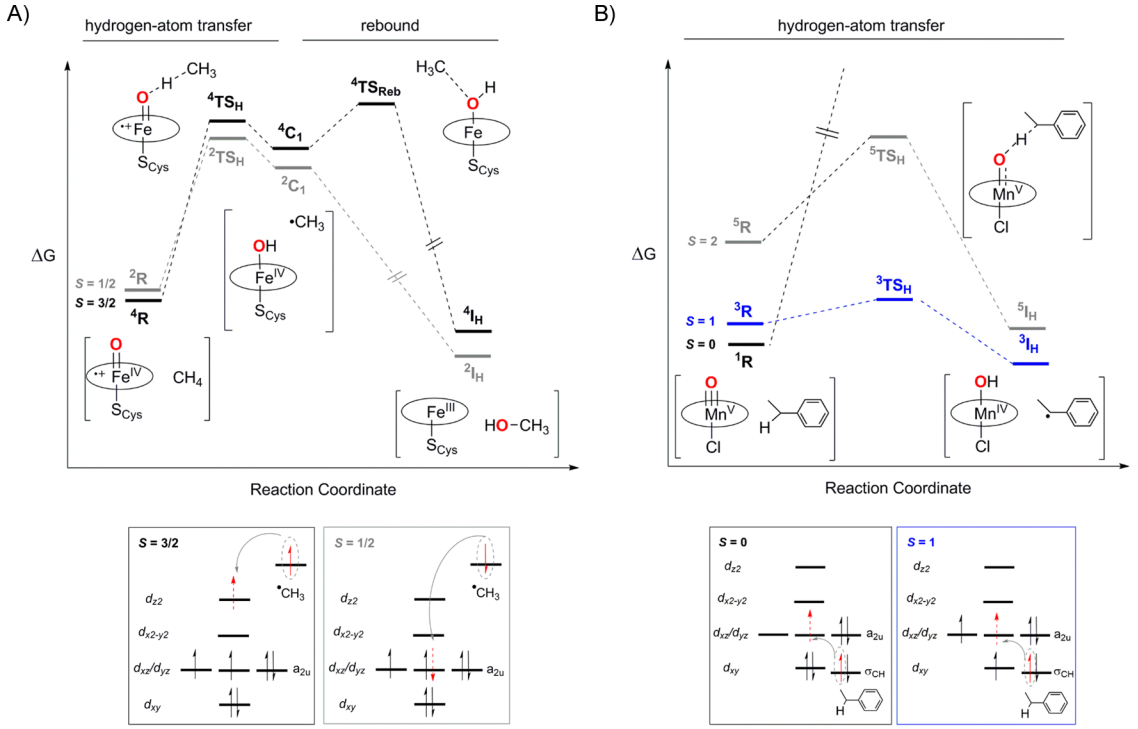

Figure 3. (A) Energy profile and reaction coordinate for the methane hydroxylation reaction by an oxoiron(IV) porphyrin π-cation radical species. Reprinted with permission from ref 58. Copyright 2017 Springer Nature. (B) Energy profile and reaction coordinate for the C−H activation by an oxomanganese(V) porphyrin complex. Reprinted with permission from ref 13. Copyright 2018 American Chemical Society.

species as alternative oxidants in P450 mediated oxidation reactions.[44−46] Recently, Green and co-workers were eventually successful in stabilizing the Cpd-I of CYP119 by using rapid freeze-quench techniques and established its catalytic competence by demonstrating its ability to oxidize unactivated hydrocarbons with an apparent second-order rate constant of $k_{app} = 1.1 \times 10^7\ M^{-1}\ s^{-1}$.[39] A large KIE of 12.5 was determined for the hydrogen-atom transfer (HAT) reaction, whose magnitude supports a mechanism in which Cpd-I abstracts a hydrogen atom from substrates, forming hydroxoiron(IV) (e.g., compound-II (Cpd-II)) that rapidly combines with a substrate radical to yield a hydroxylated product; this is called the oxygen-rebound mechanism proposed by Groves and co-workers.[13,47−49] Furthermore, the electronic structure of the CYP119 Cpd-I intermediate was confirmed to be an oxoiron(IV) porphyrin π-cation radical based on the near-zero isomer-shift in the Mössbauer spectrum, the doublet electronic ground state in the electron paramagnetic resonance spectrum, and the weekend and blue-shifted Soret band in the UV−vis, as well as a long-wavelength absorbance in the visible near 700 nm.[39] Groves and co-workers recently stabilized a second Cpd-I intermediate for the extracellular heme-thiolate aromatic peroxygenase (APO), which like CYP119 Cpd-I also showed a high reactivity for the C−H bond hydroxylation up to 100 kcal mol^{-1} with the rates of $10-10^5\ M^{-1}\ s^{-1}$.[50] The high reactivity of the Cpd-Is of the CYP119 and APO enzymes has been attributed to their highly basic Cpd-IIs as evident from the experimentally determined large pK_a's of 12.0 and 10.0, respectively.[51,52] Notably, a more basic ferryl in Cpd-II translates into a stronger $Fe^{IV}O$−H bond according to the Bordwell's equation,[51−53] thus increasing the driving force for HAT from the substrate. Accordingly, Green and co-workers proposed that the role of the cysteine thiolate in P450 catalysis is to make P450 Cpd-II more basic than a typical metal-oxo species by pushing electron density onto the ferryl oxygen.[51] This would allow for the cleavage of strong C−H bonds at biologically viable reduction potentials without damaging the protein scaffold.

Synthetic Model Complexes. The first high-valent oxoiron porphyrin complex $[(TMP^{+\bullet})Fe^{IV}(O)Cl]$ (Figure 2, Synthetic model systems, Heme) was synthesized in 1981 by Groves and co-workers via oxidation of $[(TMP)Fe^{III}(Cl)]$ (TMP = *meso*-tetramesitylporphinato dianion) with *meta*-chloroperbenzoic acid in a dichloromethane-methanol mixture at −78 °C.[29] The electronic structure was best described in terms of an overall quartet (S_t = 3/2) ground state, arising from a ferromagnetic coupling of the S = 1 iron(IV) center with a porphyrin π-cation radical (S = 1/2). This is in contrast to the S_t = 1/2 ground state determined for the P450 Cpd-I intermediate,[39] where an antiferromagnetic interaction between the iron(IV) and the porphyrin π-cation radical center was predominant. Successful generation of a number of oxoiron(IV) porphyrin π-radicals bearing electron-rich and -deficient porphyrins has been achieved subsequently.[54−58] Interestingly, a ground S_t = 3/2 state has been determined for all these intermediates; however, the extent of the ferromagnetic interaction between the iron(IV) and porphyrin π-cation radical center is strongly dependent on the *meso* and pyrole-β positions of the porphyrin ligand.[13] These experimental findings suggest a facile interconversion between the doublet and the quartet spin states of Cpd-I.

The availability of different spin states in the oxoiron(IV) porphyrin π-cation radical cores may lead to spin crossover along the reaction coordinate from reactants to products during Cpd-I mediated oxidation reactions. This concept was first proposed by Shaik, Schröder, and Schwarz in the C−H hydroxylation by Cpd-I and termed "two-state reactivity (TSR)" or "multistate reactivity (MSR)".[59−61] For example,

DOI: 10.1021/acscentsci.8b00698
ACS Cent. Sci. 2019, 5, 13−28

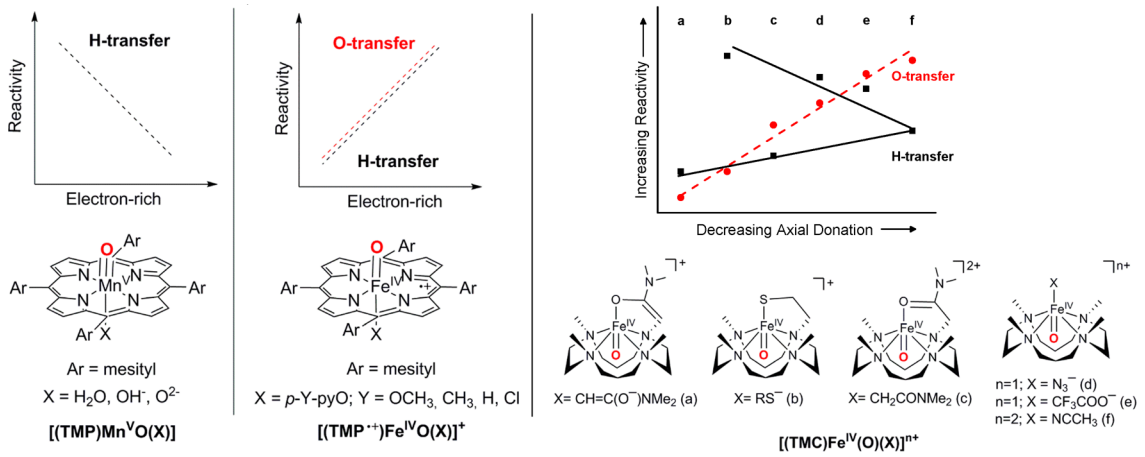

Figure 4. Axial ligand effects on the O-transfer and H-transfer reactions by $[(TMP)Mn^{V}(O)(X)]$, $[(TMP^{+\bullet})Fe^{IV}(O)(X)]^{+}$, and $[(TMC)Fe^{IV}(O)(X)]^{n+}$. Reprinted with permission from refs 31 and 67. Copyright 2016 and 2009 WILEY-VCH Verlag GmbH, respectively.

density functional theory (DFT) analysis of methane hydroxylation by an oxoiron(IV) porphyrin π-cation radical intermediate investigated the possibility of the involvement of both the $S = 3/2$ and $S = 1/2$ states in the HAT and oxygen-rebound steps (Figure 3A). While both the high-spin (HS) and low-spin (LS) pathways showed similar energy barriers for HAT, the HS pathway exhibited a larger barrier for the rebound step. In the HS state, the unpaired electron of the radical goes into a higher energy $3d_{z^2}$ orbital of the $S = 1$ Fe^{IV}–OH core of Cpd-II, whereas in the LS state the electron transfers into a lower energy singly occupied d_{xz} (or d_{yz}) orbital.

The C–H bond activation mediated by oxomanganese(V) porphyrin represents another example of potential TSR in metalloporphyrin-mediated reactions (Figure 3B).[62] DFT calculations predicted a much higher barrier for the HAT step in the singlet state ($S = 0$) as compared to that in the triplet ($S = 1$) or quintet ($S = 2$) state; this is the result of the exchange enhanced reactivity at the $S = 2$ or $S = 1$ surface. Since a singlet ground state has been determined for all oxomanganese(V) porphyrins characterized to date,[63] a spin crossing to the triplet/quintet energy surface is expected during the C–H activation reaction. Consistent with these predictions, electron-withdrawing *meso*-substituents on the porphyrin dramatically decreased the reactivity of oxomanganese(V) porphyrins because of the stabilization of the $S = 0$ ground state.[64] In contrast, for oxoiron(IV) porphyrin π-cation radicals, a different reactivity trend was observed; introduction of electron-withdrawing *meso*-substituents was shown to increase the reduction potential of Cpd-I greatly, thereby increasing the thermodynamic driving force of HAT.[65] For example, a highly electron-withdrawing Cpd-I intermediate $[(TMPyP)Fe^{IV}(O)(H_2O)]^{+}$ (TMPyP = 5,10,15,20-tetrakis(*N*-methyl-4-pyridinium)porphinato dianion) (Figure 2, Synthetic model systems, Heme) was prepared and shown to exhibit rate constants comparable to that of P450 for benzylic C–H hydroxylation reactions.[66]

A contrasting reactivity pattern has also been observed for the axial ligand effects on the reactivity of oxomanganese(V) porphyrins and oxoiron(IV) porphyrin π-cation radicals (Figure 4; left and middle).[62−64,67,68] The HAT activity of a series of axially substituted $[(TMP)Mn^{V}(O)(X)]$ (X = H_2O, OH^-, and O^{2-}) complexes is found to increase in the order of $H_2O > OH^- > O^{2-}$; this trend of decreasing reactivity with increasing electron-donation is shown to highlight the increasing energy gaps between the unreactive singlet ground state and the reactive triplet and quintet excited states on going from H_2O to OH^- and to O^{2-}.[68] In contrast, a recent study by Nam, Shaik, and co-workers demonstrated that the rates of both HAT and oxygen atom transfer (OAT) reactions of a series of $[(TMP^{+\bullet})Fe^{IV}(O)(X)]^{+}$ (X = *p*-Y-pyO; Y = OCH_3, CH_3, H, and Cl) and $[(TMP^{+\bullet})Fe^{IV}(O)(X)]$ (X = $CF_3SO_3^-$, Cl^-, AcO^-, and OH^-) increase with increasing electron-donation from the axial ligand (Figure 4; middle).[67] It is suggested that increasing axial donation strengthens the Fe–O–H bond, thereby increasing HAT activity. In addition, that also weakens the Fe=O bond, thereby enhancing the oxo-transfer reactions. However, in a subsequent study, inconsistent with the previous suggestion, Fuji and co-workers showed that the reaction rates of a series of axially substituted Cpd-I model complexes $[(TMP^{+\bullet})Fe^{IV}(O)(X)]$ with X = nitrate (NO_3), trifluoroacetate (TFA), acetate (Ac), chloride (Cl), fluoride (F), benzoate (Bz), and hydrocinnamate (Hc) did not correlate with the Fe=O vibration or the redox potential of the oxoiron(IV) porphyrin complexes.[65,69] Surprisingly, however, a direct correlation was observed between the reaction rate constants of $[(TMP^{+\bullet})Fe^{IV}(O)(X)]$ and the redox potentials of Fe^{II}/Fe^{III} in $[(TMP)Fe^{III}(X)]$ complexes, which are the final heme species after the reaction. On the basis of these results, it was suggested that the axial ligand controls the reactivity of Cpd-I by modulating the thermodynamic stability of the iron(III) porphyrin species, but not by that of Cpd-I itself. Stronger electron-donation from the axial ligand should also increase the stability of the $[(TMP)Fe^{IV}(OH)(X)]$ species formed after the HAT step; this should decelerate the rebound step, which would facilitate the escaping of substrate radicals from the radical cage. Indeed, in the case of a manganese porphyrin, recent investigation of the rebound step in the hydroxylation of deuterated ethylbenzene has displayed more stereochemical inversion at the benzylic hydroxylation site with increasing axial donation to the manganese center.[70]

Biomimetic Catalysis. In 1979, Groves and co-workers reported the first oxidation system using $[(TPP)Fe^{III}(Cl)]$ (TPP = *meso*-tetraphenylporphinato dianion) as a catalyst for C–H hydroxylation and alkene epoxidation reactions.[71] Since then, a variety of modifications have been incorporated into the bioinspired porphyrin backbone, in an effort to understand

DOI: 10.1021/acscentsci.8b00698
ACS Cent. Sci. 2019, 5, 13−28

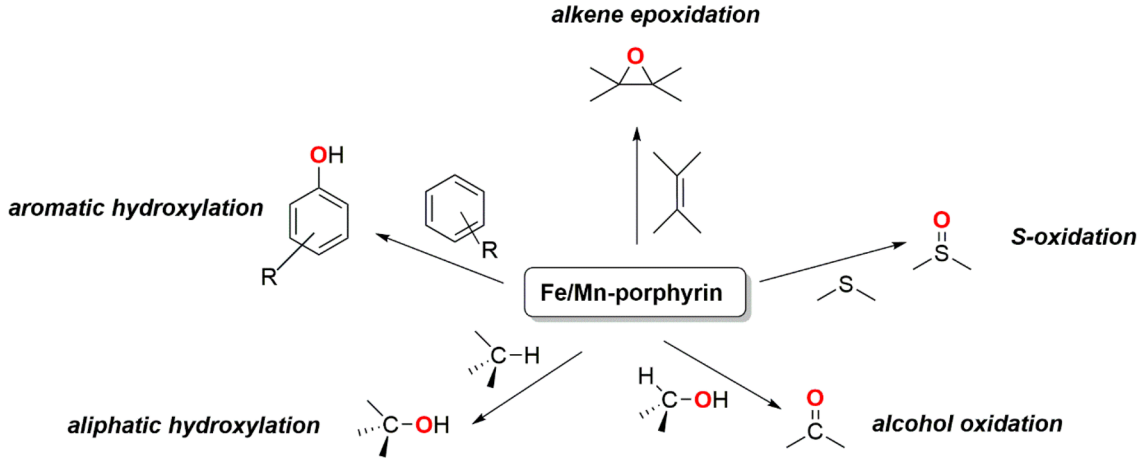

Figure 5. Oxidation reactions catalyzed by heme Fe/Mn models.

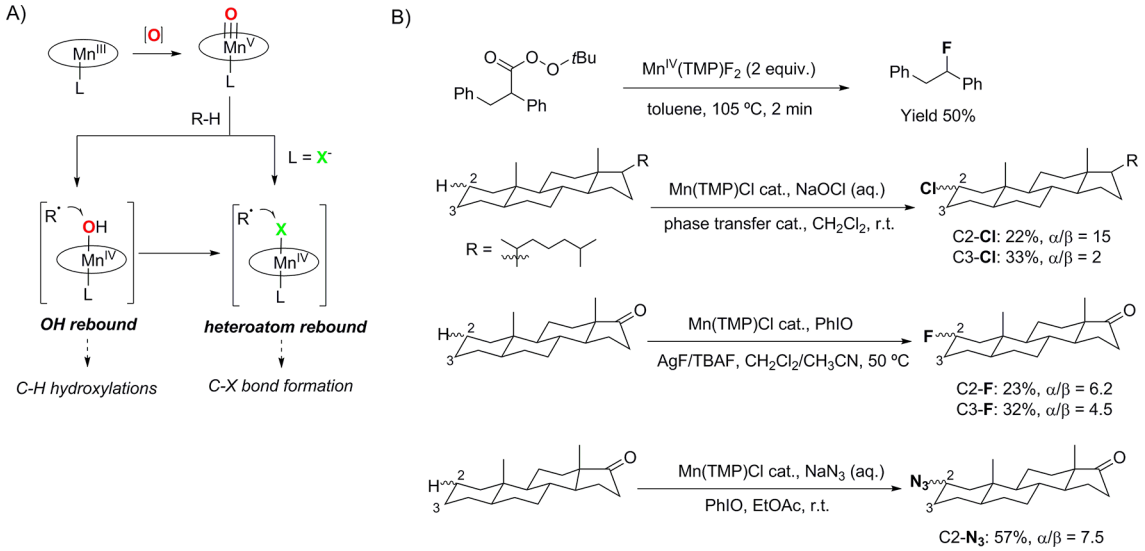

Figure 6. (A) Concept of manganese-catalyzed C−H hydroxylation and halogenation reactions via an oxygen-rebound or X-rebound mechanism. (B) Mn-catalyzed C−H halogenation and aziridination reactions.

the factors that control the catalytic efficiency.[54,56,57,72−74] In C−H oxidation reactions, the simplest metalloporphyrins without substituents at the *meso*-positions have been found to be extremely unstable against the oxidative degradation that leads to the hydroxylation at the *meso*-position; this eventually leads to the inefficiency of catalytic activity.[75] It has been subsequently demonstrated that introduction of phenyl or related groups at the *meso*-positions is a good strategy, which provides efficient catalytic oxidations by protecting these sites. Furthermore, based on the observed higher reactivity of the Cpd-I intermediates in the presence of the electron-withdrawing *meso*-substituents on the porphyrin, catalytic oxidation reactions were also tried in the presence of *meso*-phenyl substituted metalloporphyrins bearing electron-withdrawing groups, such as $[(TPFPP)Fe^{III}]^+$ (TPFPP = *meso*-tetrakis(pentafluorophenyl)porphinato dianion) and $[(TDCPP)Fe^{III}]^+$ (TDCPP = *meso*-tetrakis(2,6-dichlorophenyl)porphinato dianion).[58,74] Some of these second generation porphyrin catalysts involving electron-withdrawing *meso*-substituents have shown high reactivities in oxidation for scalable synthetic transformations of great interest for industry and academics (Figure 5).[54,56] They cover a wide variety of catalytic oxidation reactions, such as epoxidation, sulfoxidation, alcohol oxidation, arene hydroxylation, and aliphatic C−H functionalization reactions. The oxygen donors typically employed in these reactions include sodium hypochlorite, iodosylbenzene (PhIO), alkyl hydroperoxides, hydrogen peroxide, and dioxygen. Among them, dioxygen is undoubtedly the most attractive oxidant; however, additional two-electrons and two-protons are required for the reduction of the second oxygen atom of dioxygen to water in the stoichiometric monooxygenase-mediated oxygenation reactions. Accordingly, the use of additional coreductants is necessary in oxidation reactions catalyzed by metalloporphyrins and dioxygen. These coreductants can be porphyrin itself,[76] as has been demonstrated in a few metalloporphyrin-catalyzed epoxidation and C−H hydroxylation reactions, where the presence of external reductants is not a prerequisite for achieving catalysis.

The importance of a systematic mechanistic study in the design of bioinspired catalysis is well represented in the development of aliphatic C−H halogenation or aziridination reactions catalyzed by manganese porphyrin complexes (Figure 6).[13,35,70,77,78] Notably, all these reactions share common mechanistic features; they are all initiated by HAT via

DOI: 10.1021/acscentsci.8b00698
ACS Cent. Sci. 2019, 5, 13−28

oxomanganese(V) intermediates, leading to the formation of hydroxomanganese(IV) and alkyl radicals (Figure 6A).[35,77] As noted above, in the presence of strong anionic axial ligands such as F^-, Cl^-, and N_3^-, the oxygen-rebound can be suppressed, thus preventing the hydroxylation step.[35,77] In the absence of an oxygen-rebound, the alkyl radical is trapped by the $Mn^{IV}-X$ (X = Cl^-, F^-, and N_3^-) bonds, leading to the formation of C−Cl, C−F, or $C-N_3$ products with high stereo- and regioselectivity (Figure 6B). The relative rates of the OH- vs X-rebound is crucial for the success of the nonoxygenation reactivity; for example, changing to iron porphyrins, which are known to perform very fast OH-rebound, suppress the nonoxygenation reactivity, thereby yielding mainly hydroxylation products.[70]

Mononuclear nonheme oxoiron(IV) intermediates were captured and characterized in biological and abiological reactions in 2003.

3. NONHEME SYSTEMS

Biological Intermediates. Taurine α-KG dioxygenase (TauD) is the first mononuclear nonheme iron enzyme showing the formation of an oxoiron(IV) intermediate (TauD-*J*) as an active oxidizing species, which has been characterized by various spectroscopic techniques.[79,80] For example, Mössbauer characterization of a rapid-freeze-quenched sample of TauD-*J* generated in the reaction of O_2 with TauD-α-KG-taurine complex revealed a high-spin (S = 2) Fe^{IV} center with an isomer shift (δ) of 0.30 mm s^{-1}, quadrupole splitting of −0.90 mm s^{-1} and a trend of three large negative A (A_x, A_y, A_z) tensors of −18.4 T, −17.6 T, and −31 T, respectively.[80] Notably, the Mössbauer characterization of the Cpd-I intermediate in P450,[39] in contrast, revealed a trend of two large and one small negative A (A_x, A_y, A_z) tensors of −20 T, −23 T, and −3 T, respectively, which are characteristic of a low-spin (S = 1) Fe^{IV} center. The presence of a terminal Fe=O group in TauD-*J* was subsequently proved by the identification of an ^{18}O-sensitive vibration at 821 cm^{-1} in the resonance Raman spectrum and the presence of a short Fe−O distance of 1.62 Å in EXAFS studies.[81,82] Related Fe^{IV}=O intermediates,[79,83] with Mössbauer parameters comparable to TauD-*J*, were subsequently detected in the catalytic cycles of other α-KG-dependent enzymes (prolyl-4-hydroxylase, halogenases (cytochrome c_3 halogenases with chlorine or bromine and SyrB2 halogenase), desaturases (4′-methoxyviridicatin synthase), and epimerases (carbapenem synthase)) and pterin-dependent hydroxylases (tyrosine (TyrH) and phenylalanine (PheH) hydroxylases). For all the α-KG-dependent enzymes, large kinetic isotope effects (KIEs) of >50 were determined for the decay of the Fe^{IV}=O intermediates in the presence of deuterated substrates, which confirmed the participation of the oxoiron(IV) intermediates in HAT reactions (Figure 1B).[84] The HAT step is then followed by a rapid oxygen-rebound in hydroxylases, a formation of a carbon−halogen bond in halogenases (containing a halide ligand adjacent to the hydroxide on the iron center), or a second HAT step in desaturases leading to two-electron oxidation of the substrates. For the redox-neutral epimerization reaction, however, the Fe^{IV}=O intermediate is found to be responsible for the one-electron oxidation of the substrate, which is necessary to initiate the epimerization process.

The spectroscopically trapped Fe^{IV}=O intermediates of the pterin-dependent hydroxylases,[85−87] such as PheH and TyrH, are responsible for introducing a hydroxyl group at a specific position on the aromatic ring of the different amino acids. An electrophilic attack of the Fe^{IV}=O intermediates to the aromatic ring is proposed, which is supported by the observation of an inverse KIE and an NIH-shift during the hydroxylation of site-specifically deuterated aromatic substrates by PheH and TrypH.[85] In addition to the aromatic hydroxylation, the pterin-dependent hydroxylases can also perform hydroxylation of aliphatic C−H bonds on non-native substrates; KIEs larger than nonclassical values have been determined in those cases again, confirming the participation of the Fe^{IV}=O intermediates in the HAT step.[88] As evident from the above discussion, nonheme Fe^{IV}=O intermediates are primarily used in biology for HAT reactions. However, other relatively less common reactions, like epoxidation and endoperoxide formations,[89,90] are also noted for nonheme Fe^{IV}=O intermediates; thus, nonheme oxygenases, like their heme counterparts, represent another example of nature's tendency of generating similar active oxidants to perform different metabolically important transformations.

Synthetic Model Complexes. The diversified reactivity exhibited by the nonheme iron oxygenases (Figure 1B; Oxoiron(IV)-mediated oxidations) has inspired extensive efforts to mimic their high-valent oxoiron intermediates and emulate their reactivities. Wieghardt and co-workers reported the first generation of a mononuclear nonheme oxoiron(IV) complex by the ozonolysis of $[(cy\text{-}ac)Fe^{III}(CF_3SO_3)]^+$ (cy-ac = 1,4,8,11-tetraazacyclotetradecane-1-acetate) in a solvent mixture of acetone/water at −80 °C (Figure 2; Nonheme).[91] The metastable intermediate was characterized to be a low-spin (S = 1) iron(IV) species based on Mössbauer data (δ = 0.1 mm s^{-1} and ΔE_Q = 1.39 mm s^{-1}). The instability of the compound, however, prevented its further spectroscopic characterization. In a subsequent study, Münck, Nam, Que, and co-workers reported the first X-ray crystal structure of a mononuclear S = 1 oxoiron(IV) complex that was generated in the reaction of $[(TMC)Fe^{II}(CH_3CN)]^{2+}$ (TMC = 1,4,8,11-tetramethyl-1,4,8,11-tetraazacyclotetradecane) and PhIO in CH_3CN at −40 °C.[28] Since then, a large number of nonheme oxoiron(IV) complexes supported on a wide range of tetradentate and pentadentate ligands have been synthesized.[21,30−33,92] Unlike the enzymatic oxoiron(IV) cores with an S = 2 spin state, the majority of the synthesized Fe^{IV}=O cores possess an S = 1 ground state. Only a few biomimetic S = 2 oxoiron(IV) units are known that are all stabilized by enforcing a C3 symmetry about the iron(IV) center.[30,32,33]

The HAT, arene hydroxylation, and OAT reactivities of the nonheme oxoiron(IV) complexes have been investigated in significant detail by both theoretical and experimental methods.[18,21,30−32,47,93−100] So far, all theoretical studies have predicted that the Fe^{IV}=O species are better oxidants on the quintet-state than on the corresponding triplet-state.[93,96,101,102] Notably, the three most reactive oxoiron(IV) complexes in HAT and OAT reactions known to date either possess an S = 2 ground state (for example, in $[(TQA)Fe^{IV}(O)(CH_3CN)]^{2+}$, TQA = tris(2-quinolylmethyl)amine)[103] or a highly reactive S = 2 excited state that lies in close proximity to the S = 1 ground state, such as in $[(Me_3NTB)Fe^{IV}(O)]^{2+}$ (Me_3NTB = tris((*N*-methylbenzimidazol-2-yl)methyl)amine)[104] and [(TMCO)-

DOI: 10.1021/acscentsci.8b00698
ACS Cent. Sci. 2019, 5, 13−28

$Fe^{IV}(O)(CH_3CN)]^{2+}$ (TMCO = 4,8,12-trimethyl-1-oxa-4,8,12-triazacyclotetradecane)[105] (Figure 2; Nonheme). All these complexes feature extremely weak equatorial donation from the ligand that reduces the energy separation between the $d_{x^2-y^2}$ and d_{xy} orbitals, thereby stabilizing the S = 2 state. While a single state HAT is suggested to take place in the $[(TQA)Fe^{IV}(O)(CH_3CN)]^{2+}$ complex, a TSR is predominant in the S = 1 $[(Me_3NTB)Fe^{IV}(O)]^{2+}$ and $[(TMCO)Fe^{IV}(O)(CH_3CN)]^{2+}$ complexes, which presumably tunnels efficiently into the low-lying S = 2 state, thereby revealing a low energy barrier for the HAT reactivity. Conversely, strong equatorial donation from the ligand will ensure stabilization of the less reactive S = 1 state; this explains the observed sluggish reactivity of the tetracarbene oxoiron(IV) complex reported by Meyer and co-workers (Figure 2; Nonheme).[106−108] The higher reactivity of the S = 2 oxoiron(IV) core can also be extended to include arene hydroxylation reactions. Thus, although arene hydroxylation by a synthetic high-spin Fe^{IV}=O core has been reported,[32] intermediate-spin Fe^{IV}=O complexes typically do not promote such reactions. Calculations suggest that, similar to HAT reactions, the reason for the low reactivity of triplet oxoiron(IV) is the steric interaction between the incoming aromatic substrate and the equatorial ligands, which blocks access to the key π^* ($d_{xz/yz}$) acceptor orbitals on the oxoiron(IV) unit.[109−112] Consistent with this explanation, S = 1 oxoiron(IV) mediated arene hydroxylation reaction has only been recently demonstrated by properly orienting the aromatic substrate in the second coordination sphere, which enforces a linear approach of the substrate to the σ^* (d_{z^2}) orbital, thereby ensuring limited steric interaction between the Fe=O core and the substrate.[99,100,113]

The nature of the axial donation also controls the HAT reactivity of the nonheme oxoiron(IV) complexes by controlling the energies of the iron $3d_{x^2-y^2}$ and $3d_{z^2}$ orbitals.[97,98,114,115] Increasing axial donation leads to the stabilization of the $3d_{x^2-y^2}$ orbital, which provides more access to the more reactive S = 2 state by lowering the energy gap between the ground S = 1 and excited S = 2 states; this will contribute to increased HAT reactivity. At the same time, the activation barrier for HAT reaction will increase at the S = 2 surface owing to destabilization of the $3d_{z^2}$ orbital with increasing axial donation. The role of these two contrasting effects is nicely reflected in the reactivity pattern of a series of different axially substituted oxoiron(IV) complexes based on the TMC ligand. For the $[(TMC)Fe^{IV}(O)(X)]^{n+}$ (X = $NCCH_3$, CF_3COO^-, N_3^-, and RS^-) complexes, the effect of decreasing triplet-quintet energy gap with increasing axial donation compensates for the increase in the classical activation barrier, thereby leading to an antielectrophilic trend of increasing HAT reaction rates with increasing axial donation (Figure 4; right).[116] In contrast, a trend in the electrophilic reactivity is observed for the $[(TMC)Fe^{IV}(O)(CH_3CN)]^{2+}$, $[(TMC)Fe^{IV}(O)(CH_2CONMe_2)]^{2+}$, and $[(TMC)Fe^{IV}(O)(CH{=}C(O^-)NMe_2)]^{+}$ complexes (Figure 4; right), where the effect of destabilization of the d_{z^2} orbital with increasing axial donation plays a dominant role in controlling the reactivity. In addition to tune the electron-donation properties of the axial and equatorial ligands, the reactivity of the nonheme oxoiron(IV) complexes can also be controlled by adding redox-innocent Lewis acid metal ions or proton.[92,117−119] Notably, only the highly basic one-electron reduced oxoiron(III) species (and not the electrophilic oxoiron(IV) core) can interact strongly to the added metal ions or proton. This increases the thermodynamic driving force for reduction of the oxoiron(IV) core, resulting in a large positive shift of its one-electron reduction potential (E_{red}),[92,117−119] thereby attributing to the enhancement of both the HAT and OAT reaction rates.

The situation is however different for the nonheme oxomanganese(IV and V) complexes,[120−124] although a TSR concept is also applicable for rationalizing their HAT and OAT reactivities. Notably, known examples of mononuclear nonheme oxomanganese(IV) complexes (Figure 2) are all stabilized in an S = 3/2 ground state with an electronic configuration of $d_{xy}{}^1d_{xz}{}^1d_{yz}{}^1d_{x^2-y^2}{}^0d_{z^2}{}^0$.[125−129] However, the sterically less demanding σ pathway, involving electron transfer from substrate to the d_{z^2} orbital, is energetically unfavorable for HAT reactions mediated by oxomanganese(IV) complexes, as the Mn $3d_{z^2}$ orbital is destabilized relative to Fe $3d_{z^2}$ owing to the lower effective nuclear charge of manganese. Correspondingly, Mn^{IV}=O mediated HAT reactions proceed predominantly along a π-pathway[31] involving a higher activation barrier relative to the Fe^{IV}=O mediated HAT reactions. The predominance of the π reactivity also ensures that the HAT reactions mediated by Mn^{IV}=O species are controlled predominantly by steric effects. Accordingly, a contrasting reactivity pattern is observed in the HAT reactivity of the Mn^{IV}=O and Fe^{IV}=O complexes supported by the bispidine BP1 and BP2 ligands (see Figure 2 for $[(BP1)M^{IV}(O)]^{2+}$ and $[(BP2)M^{IV}(O)]^{2+}$).[130] While the higher Fe^{IV}/Fe^{III} reduction potential of the $[(BP2)Fe^{IV}(O)]^{2+}$ complex relative to $[(BP1)Fe^{IV}(O)]^{2+}$ results in faster HAT and OAT rates of the former, the corresponding $[(BP2)Mn^{IV}(O)]^{2+}$ complex is a sluggish oxidant relative to $[(BP1)Mn^{IV}(O)]^{2+}$ owing to the higher steric demand of BP2 relative to BP1. The higher steric demand of the Mn^{IV}=O mediated oxidation reactions is also reflected in the observed contrasting trends in their HAT and OAT reaction rates in the presence of Lewis- or Bronsted-acids.[131] For example, the binding of Sc^{3+} ion to the $[(N_4Py)Mn^{IV}(O)]^{2+}$ complex (N_4Py = *N,N*-bis(2-pyridylmethyl)-*N*-bis(2-pyridyl)methylamine) led to an enhancement in the OAT rates, but a deceleration of the HAT rates. While the large positive shift in the $[Mn{=}O]^{IV/III}$ reduction potential contributes to the increased OAT rates, the HAT reactions are presumably inhibited by sterics due to the binding of the Sc^{3+}/H^+ ion to the Mn^{IV}=O moiety.

> Mn^{IV}=O mediated HAT reactions proceed predominantly along a π-pathway involving a higher activation barrier relative to the Fe^{IV}=O mediated HAT reactions. The predominance of the π reactivity also ensures that the HAT reactions mediated by Mn^{IV}=O species are controlled predominantly by steric effects.

Biomimetic Catalysis. As evident from the above discussion, reactivities of the nonheme enzymatic and synthetic oxoiron(IV) complexes are attributed to the S = 2 state. The prerequisite necessary for achieving biomimetic catalysis is therefore the generation of oxoiron(IV) complexes with readily

DOI: 10.1021/acscentsci.8b00698
ACS Cent. Sci. 2019, 5, 13−28

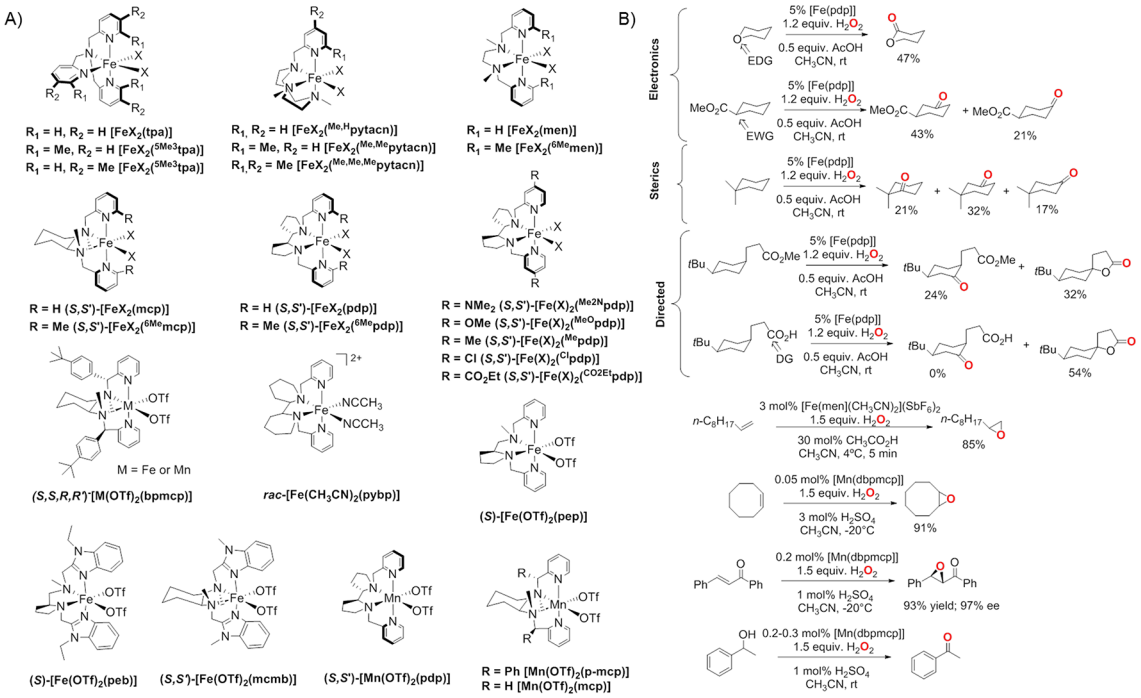

Figure 7. (A) Bioinspired Fe- and Mn-based nonheme catalysts. (B) Some examples showing the alkane hydroxylation, olefin epoxidation, and alcohol oxidation by nonheme iron and manganese catalysts and using H_2O_2 as an oxidant. Reprinted with permission from ref 140. Copyright 2017 Springer Nature.

available S = 2 state for the two-electron HAT or OAT reactions. Very recently, Long and co-workers demonstrated the achievement of a good compromise between reactivity and stability by employing metal−organic framework (MOF) to support highly reactive oxoiron moieties for catalytic C−H bond oxidation reactions under mild conditions.[132] They showed that the magnesium-diluted high-spin iron(II) centers within $Fe_{0.1}Mg_{1.9}$(dobdc) (dobdc = 2,5-dioxido-1,4-benzenedicarboxylate) can activate N_2O, most likely forming a transient high-spin oxoiron(IV) intermediate, which can undergo a rapid HAT from ethane, followed by a fast oxygen-rebound to yield ethanol with a low yield of 1% and a turnover of 1.5. DFT calculations have shown that a combination of four carboxylate and one aryloxide groups of the dobdc^{4-} linker enforces a weak field ligand at the iron center, thereby stabilizing an S = 2 spin state of the transient oxoiron(IV) core. Furthermore, the porosity of the MOF structure provides easy access of the substrate to the oxoiron(IV) unit; a combination of these two factors ensures a rapid HAT reaction with ethane. In addition, the ethyl radical formed after the HAT step undergoes a preferential oxygen-rebound, leading to the hydroxylation product with a lower energy barrier relative to the alternative desaturation (via a second HAT step) or radical dissociation (leading to secondary products) steps involving higher energy barriers. However, the DFT calculated higher-energy barrier of the dissociation step relative to hydroxylation is not consistent with the experimentally observed high-yield formation of the one-electron oxidized Fe(III)−OH product which prematurely halts the catalytic cycle, thereby limiting the yield and turnover of ethanol product.[132,133]

Controlled reductive cleavage of O_2 to form highly oxidizing oxoiron(V) species has been proposed to take place in biology.[134] For example, in Rieske dioxygenase, O_2 binding at a ferrous center followed by one-electron reduction from a nearby Rieske Fe_2S_2 cluster results in the formation of an hydroperoxoiron(III) species, which is the last species detected before substrate oxidation occurs.[135] It has been proposed that the Fe(III)-OOH species isomerizes toward an Fe^{V}(O)(OH) species, which exhibits diverse reactivities, including hydroxylation of aryl C−H bonds, epoxidation, and *cis*-dihydroxylation of arenes (Figure 1B).[2,134] Direct cycling between the iron(III) and iron(V) states can also be achieved via a shunt mechanism by employing H_2O_2 as the oxidant; no reductase components are required in this case.[136] This shunt pathway has been successfully used in catalytic C−H bond hydroxylation, epoxidation, and *syn*-dihydroxylation reactions by employing nonheme iron complexes (Figure 7).[34,36,137−139] Further, in contrast to biology, where direct evidence of the oxoiron(V) intermediate is lacking,[138] evidence for the involvement of oxoiron(V) species in chemical oxidation reactions has been accumulated recently.[138,140−143] For example, iron(II) complexes with strong field tetradentate *N*-based ligands and possessing two *cis*-labile sites are competent catalysts, which are rapidly oxidized by H_2O_2 to produce mononuclear ferric species, which in the presence of water or alkane carboxylic acids (RCOOH) can split the O−O bond in a heterolytic manner to produce high-valent electrophilic Fe^{V}(O)(OH) or Fe^{V}(O)(OOCR) oxidants, respectively (Figure 8).[34,36,142,144] A few Fe^{V}═O species have now been detected under catalytic turnover conditions and characterized by a variety of low-temperature MS, EPR, Mössbauer, and isotopic labeling studies.[138,145,146] On the basis of detailed experimental and theoretical studies, these intermediates are shown to be strong oxidants and capable of regenerating the iron(III) resting state, thereby ensuring catalytic turnovers. In reactions with olefins, Fe^{V}(O)(OH) can lead to both stereoselective epoxidation and *syn*-dihydroxylation reactions, whereas Fe^{V}(O)(OOCR) is capable of performing only stereoselective epoxidation reactions.[142] Furthermore, both

DOI: 10.1021/acscentsci.8b00698
ACS Cent. Sci. 2019, 5, 13−28

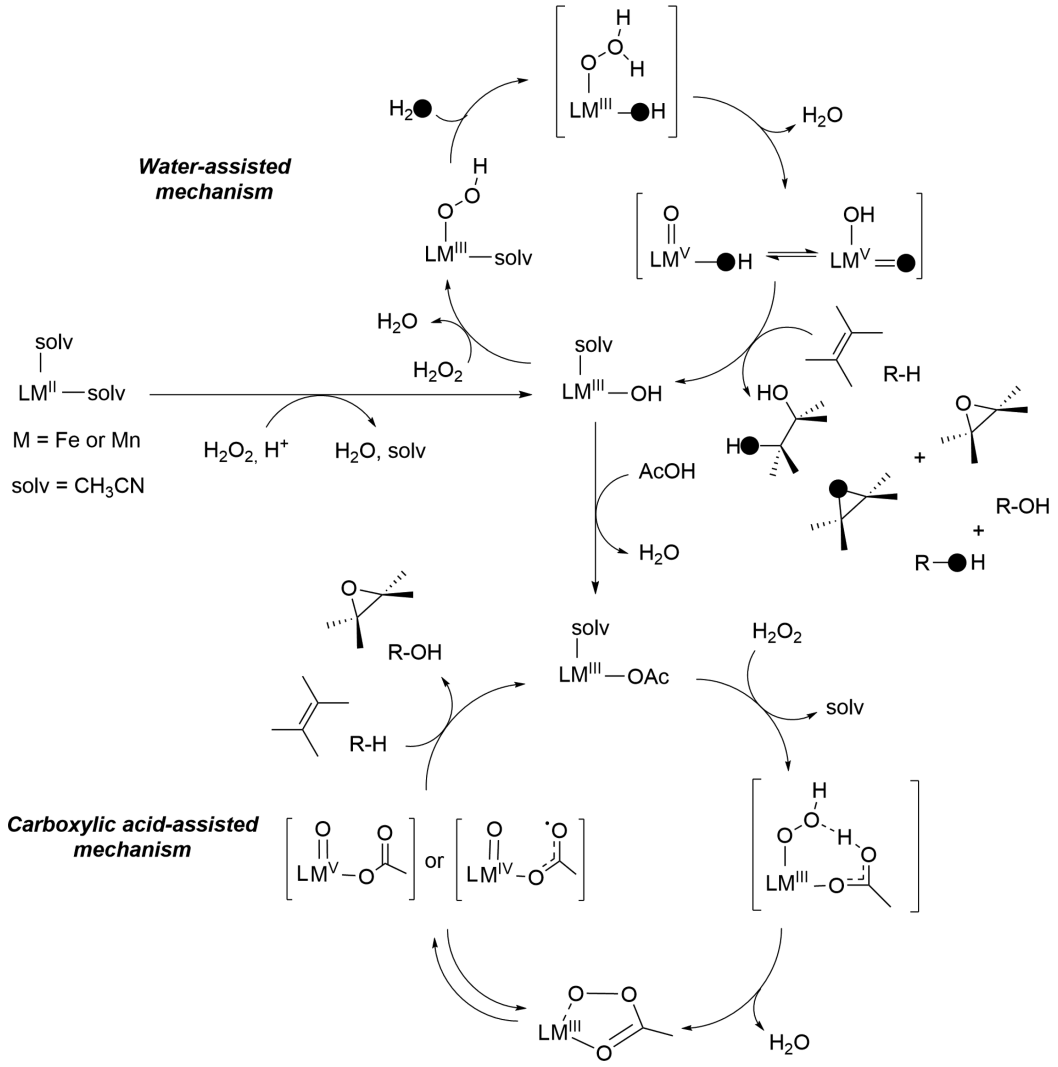

Figure 8. Proposed mechanisms for the nonheme iron and manganese complex-catalyzed oxidation reactions, such as water-assisted mechanism and carboxylic acid-assisted mechanism. Reprinted with permission from ref 140. Copyright 2017 Springer Nature.

the high-valent oxoiron(V) species are oxidants for C−H oxidation reactions, showing good selectivity toward the most electron rich C−H bonds of the substrates (Figure 7B; Electronics), as expected for highly electrophilic oxidizing species.[140] The steric bulk of the catalyst also dictates the selectivity when there are no differences in the electronic factors, favoring oxidation at the least sterically encumbered positions (Figure 7B; Sterics). Alternatively, directing groups can be employed to override the steric and electronic factors, in order to achieve oxidation at a desired position; for example, selective hydroxylation in the γ-position with eventual formation of γ-lactones by employing carboxylic acid substrates (Figure 7B; Directed).[139]

Bioinspired manganese complexes bearing nonheme ligands can also act as efficient catalysts in asymmetric epoxidation and hydroxylation reactions by employing H_2O_2 as an oxidant and carboxylic acids as an essential additive to improve product yields and stereo-, regio-, and enantioselectivities (Figure 7).[124,147−152] Similar to the iron complexes, the availability of *cis*-binding sites is a prerequisite for the "carboxylic-acid assisted" heterolytic cleavage of the O−O bond in Mn^{III}−OOH species, thereby leading to the generation of active Mn^{V}=O species.[124,147−152] Notably, manganese complexes based on pentadentate nonheme ligands can also act as efficient epoxidation catalysts using PhIO as an oxidant. Second-sphere hydrogen-bonding interaction between the hydrogen atoms of the carboxylic acid and the oxo-group of the Mn(V)=O species presumably explains the formation of a highly reactive Mn(V)=O···H species responsible for the enantioselective epoxidation reaction.[147]

Bioinspired iron and manganese complexes bearing nonheme ligands can also act as efficient catalysts in asymmetric epoxidation and hydroxylation reactions by employing H_2O_2 as an oxidant and carboxylic acids as an essential additive to improve product yields and stereo-, regio-, and enantioselectivities

DOI: 10.1021/acscentsci.8b00698
ACS Cent. Sci. 2019, 5, 13−28

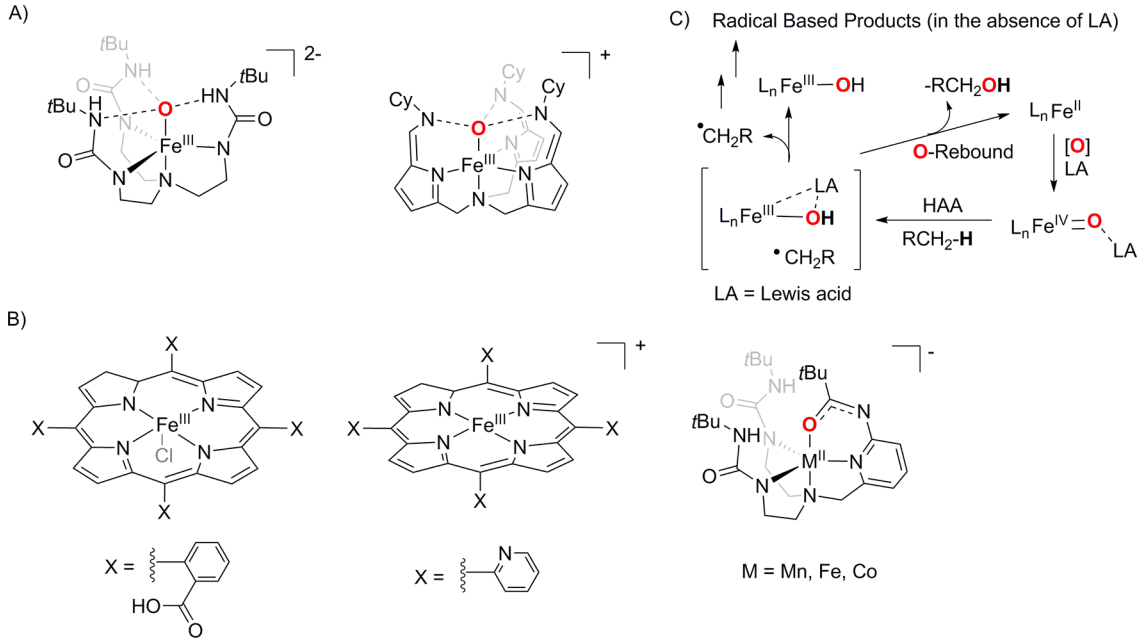

Figure 9. (A) Examples of intramolecular static H-bonding in the secondary coordination sphere leading to the stabilization of oxoiron(III) complexes. (B) Examples of complexes where intramolecular dynamic H-bonding interaction in the secondary sphere leads to the selective reduction of dioxygen to water. (C) Possible role of Lewis acids (LA) in ensuring oxoiron(IV) mediated catalytic C−H bond oxidation reactions.

4. CONCLUSION

Metalloenzymes activate dioxygen by employing earth-abundant metals and exhibit diverse reactivities in oxidation reactions, including epoxidation of olefins, oxidation of alkane C−H bonds, and *syn*-dihydroxylation of arenes. Such reactions are carried out under ambient conditions with high efficiency and high stereospecificity. Research efforts from the last two decades have led to a detailed understanding of the mechanisms of the biological oxidation reactions. Dioxygen activation occurs predominantly at an iron(II) center, which is then followed by a controlled transfer of electrons (and protons) from a reductase component to generate high-valent metal-oxo species, which are responsible for the substrate oxidation reactions. In many cases, such proton and electron transfer events are precisely controlled by noncovalent interactions between the metal center of the active site and the protein derived secondary coordination sites bearing functional groups.[153,154] Alternatively, an iron(III) resting state of the enzyme can react with H_2O_2 to form the metal-oxo species via a shunt pathway without the requirement of any reductase component.

Recently, a number of heme and nonheme iron- and manganese-oxo complexes have been synthesized in biomimetic chemistry, and many of them show intriguing reactivities, which in turn have provided vital insights into the enzymatic reactions. Notably, secondary sphere interactions have been shown to greatly influence the formation and subsequent reactivity of the metal-oxo cores. On one hand, the incorporation of static H-bonds is found to be extremely effective in stabilizing reactive species within transition metal complexes, for example, the reports of the stabilization of the unique oxoiron(III) cores upon dioxygen or N_2O activation by employing synthetic ligands (H_3buea^{3-} and $N(afa^{Cy})_3$, Figure 9A) that promote intramolecular H-bonds.[155,156] Alternatively, the use of a more dynamic secondary sphere by incorporating functional groups that can serve diverse functions such as proton and electron relays can influence the efficiency and product selectivity of the catalytic processes involving metal−oxygen species as reactive intermediates (Figure 9B). For example, the Mayer group has presented a dramatic increase in the rate and selectivity of electrocatalytic O_2 reduction to water by Fe tetra-arylporphyrin complexes; the porphyrin ligands (Porp-X_4) contain proton delivery functional groups such as carboxylic acids and pyridine to promote reduction of O_2 to water rather than hydrogen peroxide.[157−159] Similarly, the use of a nonheme $[H_2bupa]^{2-}$ ligand containing both intramolecular H-bond donating and accepting groups in the form of urea N−H groups and an anionic amidate group proved effective in the transition-metal mediated catalytic reduction of O_2 to water with modest turnover using a sacrificial hydrogen-atom source.[160,161] Further, intramolecular secondary sphere interaction of a redox-inactive Lewis acid like scandium triflate or carboxylic or Bronsted acids with metal−oxygen intermediates also led to the formation of highly electrophilic oxidants capable of catalytic hydroxylation of cyclohexane and benzene and enantioselective epoxidation of olefins.[147,162−164] These studies corroborate the proposed influence of secondary coordination effects on biological catalysis and have also helped in mimicking the oxidative reactivity of the bioenzymes by employing simple iron and manganese coordination complexes, even in the absence of the extended protein substructures surrounding the enzymes' active sites. These have opened up totally new perspectives in organic synthesis. Catalysts capable of conducting C−H and C═C oxidation reactions with high product yields and enantioselectivities amenable for high-scale industrial synthesis have been designed. In particular, recent progress in the design of catalysts responsible for enantioselective oxidation of hydrocarbons and *syn*-dihydroxylation of alkenes is promising and opens up options to replace the industrially used high-valent metal-oxides, like OsO_4, RuO_4, or MnO_4^-, which are either very toxic or lead to over oxidation of most substrates.[165]

DOI: 10.1021/acscentsci.8b00698
ACS Cent. Sci. 2019, 5, 13−28

There are, nevertheless, still some gaps in our present understanding of the chemistry of the reductive dioxygen reaction at transition metal centers for substrate oxidation reactions. In particular, the mechanistic scenario leading to a preferential olefin *syn*-dihydroxylation reaction (over epoxidation reaction) is not well understood. High-spin Fe^{III}−OOH or Fe^{II}−OOH species have been proposed as alternative nucleophilic oxidants that lead to preferential *syn*-dihydroxylation reactions; however, conclusive evidence is lacking, which makes the mechanism ambiguous.[166] Moreover, although several examples of catalytic dioxygen activation reactions at heme iron and manganese centers are known, most of the catalytic systems involving nonheme metal complexes employ H_2O_2 as the oxidant. The use of O_2 in catalytic oxidation reactions is difficult owing to the challenges associated with the addition of sacrificial reductants required to couple the $4e^-$ reduction of O_2 with that of the $2e^-$ oxidation of substrates. Although some strategies have been put forward with the aim of developing oxidation methods that employ O_2 as oxidant,[166] the yields of the oxidized products reported in these studies are still too low for practical use. Further, in spite of the predominance of the oxoiron(IV) cores in biology,[1,13,16−19] intermediacy of such cores in catalytic epoxidation and aliphatic C−H functionalization reactions by nonheme iron complexes remains elusive. In addition, although synthetic nonheme iron catalysts for arene-hydroxylation reactions are reported, the nature of the active intermediate(s) has been controversially discussed as both Fe^{IV}=O and Fe^{V}=O species in the absence of direct spectroscopic evidence. In the context of catalytic C−H bond activation reactions, the reaction is proposed to be initiated by a rate determining H-atom abstraction step by Fe^{IV}=O species, followed by an oxygen-rebound between the resulting [Fe^{III}(OH)] and substrate radical species (Figure 9C). In this oxygen-rebound mechanism,[71] the formal oxidation state of metal should be reduced by $2e^-$ to Fe^{2+}, and the product formed will then be alcohol. The Fe^{2+} product can be reoxidized to Fe^{IV}=O in the presence of an oxidant leading to catalytic reactions. However, for nonheme oxoiron(IV) model complexes, the dissociation of the substrate radical formed via HAT from hydrocarbons is more favored than the oxygen-rebound process, leading to one electron reduced metal complex products resulting in noncatalytic oxidation reactions.[92] One way to deal with this problem will be to enforce Lewis acidic interaction to the Fe^{IV}=O cores via modification of the secondary coordination sphere, which will make the iron center electrophilic and will help to speed up the rebound step and ensure a two-electron chemistry, thereby assuring catalysis (Figure 9C). Thus, new and innovative synthetic strategies are needed to generate transition metal complexes that can efficiently use O_2 as the terminal oxidant, in order to achieve challenging oxidation of substrates like functionalization of C−H bonds and *syn*-dihydroxylation of arenes.

AUTHOR INFORMATION

Corresponding Authors

*(K.R.) E-mail: kallol.ray@chemie.hu-berlin.de.

*(W.N.) E-mail: wwnam@ewha.ac.kr.

ORCID

Kallol Ray: 0000-0003-2074-8844

Wonwoo Nam: 0000-0001-8592-4867

Author Contributions

#M.G. and T.C. contributed equally to this work.

Notes

The authors declare no competing financial interest.

ACKNOWLEDGMENTS

The authors gratefully acknowledge the contributions of their collaborators and co-workers in the cited references, and the financial support by the NRF of Korea through CRI (NRF-2012R1A3A2048842 to W.N.) and GRL (NRF-2010-00353 to W.N.). K.R. thanks the Deutsche Forschungsgemeinschaft (UniCat; EXC 314-2 and Heisenberg Professorship). T.C. gratefully acknowledges the Alexander von Humboldt Foundation for a postdoctoral fellowship.

REFERENCES

(1) Sahu, S.; Goldberg, D. P. Activation of Dioxygen by Iron and Manganese Complexes: A Heme and Nonheme Perspective. *J. Am. Chem. Soc.* **2016**, *138*, 11410−11428.

(2) Kovaleva, E. G.; Lipscomb, J. D. Versatility of Biological Non-Heme Fe(II) Centers in Oxygen Activation Reactions. *Nat. Chem. Biol.* **2008**, *4*, 186−193.

(3) Pau, M. Y. M.; Lipscomb, J. D.; Solomon, E. I. Substrate Activation for O_2 Reactions by Oxidized Metal Centers in Biology. *Proc. Natl. Acad. Sci. U. S. A.* **2007**, *104*, 18355−18362.

(4) Jones, R. D.; Summerville, D. A.; Basolo, F. Synthetic Oxygen Carriers Related to Biological Systems. *Chem. Rev.* **1979**, *79*, 139−179.

(5) Wood, P. M. The Potential Diagram for Oxygen at pH 7. *Biochem. J.* **1988**, *253*, 287−289.

(6) Que, L., Jr. 60 Years of Dioxygen Activation. *J. Biol. Inorg. Chem.* **2017**, *22*, 171−173.

(7) Nam, W. Dioxygen Activation by Metalloenzymes and Models. *Acc. Chem. Res.* **2007**, *40*, 465−465.

(8) Fukuzumi, S.; Lee, Y.-M.; Nam, W. Mechanisms of Two-Electron versus Four-Electron Reduction of Dioxygen Catalyzed by Earth-Abundant Metal Complexes. *ChemCatChem* **2018**, *10*, 9−28.

(9) Zhang, W.; Lai, W.; Cao, R. Energy-Related Small Molecule Activation Reactions: Oxygen Reduction and Hydrogen and Oxygen Evolution Reactions Catalyzed by Porphyrin- and Corrole-Based Systems. *Chem. Rev.* **2017**, *117*, 3717−3797.

(10) Nastri, F.; Chino, M.; Maglio, O.; Bhagi-Damodaran, A.; Lu, Y.; Lombardi, A. Design and Engineering of Artificial Oxygen-Activating Metalloenzymes. *Chem. Soc. Rev.* **2016**, *45*, 5020−5054.

(11) Hematian, S.; Garcia-Bosch, I.; Karlin, K. D. Synthetic Heme/Copper Assemblies: Toward an Understanding of Cytochrome c Oxidase Interactions with Dioxygen and Nitrogen Oxides. *Acc. Chem. Res.* **2015**, *48*, 2462−2474.

(12) Jasniewski, A. J.; Que, L., Jr. Dioxygen Activation by Nonheme Diiron Enzymes: Diverse Dioxygen Adducts, High-Valent Intermediates, and Related Model Complexes. *Chem. Rev.* **2018**, *118*, 2554−2592.

(13) Huang, X.; Groves, J. T. Oxygen Activation and Radical Transformations in Heme Proteins and Metalloporphyrins. *Chem. Rev.* **2018**, *118*, 2491−2553.

(14) Solomon, E. I.; Goudarzi, S.; Sutherlin, K. D. O_2 Activation by Non-Heme Iron Enzymes. *Biochemistry* **2016**, *55*, 6363−6374.

(15) Poulos, T. L. Heme Enzyme Structure and Function. *Chem. Rev.* **2014**, *114*, 3919−3962.

(16) Abu-Omar, M. M.; Loaiza, A.; Hontzeas, N. Reaction Mechanisms of Mononuclear Non-Heme Iron Oxygenases. *Chem. Rev.* **2005**, *105*, 2227−2252.

(17) Solomon, E. I.; Brunold, T. C.; Davis, M. I.; Kemsley, J. N.; Lee, S.-K.; Lehnert, N.; Neese, F.; Skulan, A. J.; Yang, Y.-S.; Zhou, J. Geometric and Electronic Structure/Function Correlations in Non-Heme Iron Enzymes. *Chem. Rev.* **2000**, *100*, 235−350.

DOI: 10.1021/acscentsci.8b00698
ACS Cent. Sci. 2019, 5, 13−28

(18) Ray, K.; Pfaff, F. F.; Wang, B.; Nam, W. Status of Reactive Non-Heme Metal−Oxygen Intermediates in Chemical and Enzymatic Reactions. *J. Am. Chem. Soc.* **2014**, *136*, 13942−13958.
(19) Solomon, E. I.; Light, K. M.; Liu, L. V.; Srnec, M.; Wong, S. D. Geometric and Electronic Structure Contributions to Function in Non-heme Iron Enzymes. *Acc. Chem. Res.* **2013**, *46*, 2725−2739.
(20) Roach, P. L.; Clifton, I. J.; Hensgens, C. M. H.; Shibata, N.; Schofield, C. J.; Hajdu, J.; Baldwin, J. E. Structure of Isopenicillin*N* Synthase Complexed with Substrate and the Mechanism of Penicillin Formation. *Nature* **1997**, *387*, 827−830.
(21) Nam, W. Synthetic Mononuclear Nonheme Iron−Oxygen Intermediates. *Acc. Chem. Res.* **2015**, *48*, 2415−2423.
(22) Hong, S.; Sutherlin, K. D.; Park, J.; Kwon, E.; Siegler, M. A.; Solomon, E. I.; Nam, W. Crystallographic and Spectroscopic Characterization and Reactivities of A Mononuclear Non-Haem Iron(III)-Superoxo Complex. *Nat. Commun.* **2014**, *5*, 5440−5446.
(23) Chiang, C.-W.; Kleespies, S. T.; Stout, H. D.; Meier, K. K.; Li, P.-Y.; Bominaar, E. L.; Que, L., Jr.; Münck, E.; Lee, W.-Z. Characterization of a Paramagnetic Mononuclear Nonheme Iron-Superoxo Complex. *J. Am. Chem. Soc.* **2014**, *136*, 10846−10849.
(24) Bang, S.; Lee, Y.-M.; Hong, S.; Cho, K.-B.; Nishida, Y.; Seo, M. S.; Sarangi, R.; Fukuzumi, S.; Nam, W. Redox-Inactive Netal Ions Modulate the Reactivity and Oxygen Release of Mononuclear Non-Haem Iron(III)−Peroxo Complexes. *Nat. Chem.* **2014**, *6*, 934−940.
(25) Cho, J.; Jeon, S.; Wilson, S. A.; Liu, L. V.; Kang, E. A.; Braymer, J. J.; Lim, M. H.; Hedman, B.; Hodgson, K. O.; Valentine, J. S.; Solomon, E. I.; Nam, W. Structure and Reactivity of A Mononuclear Non-Haem Iron(III)−Peroxo Complex. *Nature* **2011**, *478*, 502−505.
(26) de Oliveira, F. T.; Chanda, A.; Banerjee, D.; Shan, X.; Mondal, S.; Que, L., Jr.; Bominaar, E. L.; Münck, E.; Collins, T. J. Chemical and Spectroscopic Evidence for an Fe^{V}-Oxo Complex. *Science* **2007**, *315*, 835−838.
(27) Bukowski, M. R.; Koehntop, K. D.; Stubna, A.; Bominaar, E. L.; Halfen, J. A.; Münck, E.; Nam, W.; Que, L., Jr. A Thiolate-Ligated Nonheme Oxoiron(IV) Complex Relevant to Cytochrome P450. *Science* **2005**, *310*, 1000−1002.
(28) Rohde, J.-U.; In, J.-H.; Lim, M. H.; Brennessel, W. W.; Bukowski, M. R.; Stubna, A.; Münck, E.; Nam, W.; Que, L., Jr. Crystallographic and Spectroscopic Characterization of a Nonheme Fe(IV)═O Complex. *Science* **2003**, *299*, 1037−1039.
(29) Groves, J. T.; Haushalter, R. C.; Nakamura, M.; Nemo, T. E.; Evans, B. J. High-Valent Iron-Porphyrin Complexes related to Peroxidase and Cytochrome P-450. *J. Am. Chem. Soc.* **1981**, *103*, 2884−2886.
(30) Puri, M.; Que, L., Jr. Toward the Synthesis of More Reactive S = 2 Non-Heme Oxoiron(IV) Complexes. *Acc. Chem. Res.* **2015**, *48*, 2443−2452.
(31) Engelmann, X.; Monte-Pérez, I.; Ray, K. Oxidation Reactions with Bioinspired Mononuclear Non-Heme Metal−Oxo Complexes. *Angew. Chem., Int. Ed.* **2016**, *55*, 7632−7649.
(32) Bigi, J. P.; Harman, W. H.; Lassalle-Kaiser, B.; Robles, D. M.; Stich, T. A.; Yano, J.; Britt, R. D.; Chang, C. J. A High-Spin Iron(IV)−Oxo Complex Supported by a Trigonal Nonheme Pyrrolide Platform. *J. Am. Chem. Soc.* **2012**, *134*, 1536−1542.
(33) England, J.; Martinho, M.; Farquhar, E. R.; Frisch, J. R.; Bominaar, E. L.; Münck, E.; Que, L., Jr. A Synthetic High-Spin Oxoiron(IV) Complex: Generation, Spectroscopic Characterization, and Reactivity. *Angew. Chem., Int. Ed.* **2009**, *48*, 3622−3626.
(34) Oloo, W. N.; Que, L., Jr. Bioinspired Nonheme Iron Catalysts for C-H and C = C Bond Oxidation: Insights into the Nature of the Metal-Based Oxidants. *Acc. Chem. Res.* **2015**, *48*, 2612−2621.
(35) Liu, W.; Groves, J. T. Manganese Catalyzed C−H Halogenation. *Acc. Chem. Res.* **2015**, *48*, 1727−1735.
(36) Cussó, O.; Ribas, X.; Costas, M. Biologically Inspired Non-Heme Iron-Catalysts for Asymmetric Epoxidation; Design Principles and Perspectives. *Chem. Commun.* **2015**, *51*, 14285−14298.
(37) Yosca, T. H.; Green, M. T. Preparation of Compound I in P450cam: the Prototypical P450. *Isr. J. Chem.* **2016**, *56*, 834−840.
(38) Krest, C. M.; Silakov, A.; Rittle, J.; Yosca, T. H.; Onderko, E. L.; Calixto, J. C.; Green, M. T. Significantly Shorter Fe−S Bond in Cytochrome P450-I Is Consistent with Greater Reactivity Relative to Chloroperoxidase. *Nat. Chem.* **2015**, *7*, 696−702.
(39) Rittle, J.; Green, M. T. Cytochrome P450 Compound I: Capture, Characterization, and C-H Bond Activation Kinetics. *Science* **2010**, *330*, 933−937.
(40) Egawa, T.; Shimada, H.; Ishimura, Y. Evidence for Compound I Formation in the Reaction of Cytochrome-P450cam with *m*-Chloroperbenzoic Acid. *Biochem. Biophys. Res. Commun.* **1994**, *201*, 1464−1469.
(41) Green, M. T. The Structure and Spin Coupling of Catalase Compound I: A Study of Noncovalent Effects. *J. Am. Chem. Soc.* **2001**, *123*, 9218−9219.
(42) Khindaria, A.; Aust, S. D. EPR Detection and Characterization of Lignin Peroxidase Porphyrin π-Cation Radical. *Biochemistry* **1996**, *35*, 13107−13111.
(43) Patterson, W. R.; Poulos, T. L.; Goodin, D. B. Identification of a Porphyrin π Cation Radical in Ascorbate Peroxidase Compound I. *Biochemistry* **1995**, *34*, 4342−4345.
(44) Chandrasena, R. E. P.; Vatsis, K. P.; Coon, M. J.; Hollenberg, P. F.; Newcomb, M. Hydroxylation by the Hydroperoxy-Iron Species in Cytochrome P450 Enzymes. *J. Am. Chem. Soc.* **2004**, *126*, 115−126.
(45) Newcomb, M.; Aebisher, D.; Shen, R.; Chandrasena, R. E. P.; Hollenberg, P. F.; Coon, M. J. Kinetic Isotope Effects Implicate Two Electrophilic Oxidants in Cytochrome P450-Catalyzed Hydroxylations. *J. Am. Chem. Soc.* **2003**, *125*, 6064−6065.
(46) Nam, W.; Ryu, Y.; Song, W. Oxidizing Intermediates in Cytochrome P450 Model Reactions. *J. Biol. Inorg. Chem.* **2004**, *9*, 654−660.
(47) Cho, K.-B.; Hirao, H.; Shaik, S.; Nam, W. To Rebound or Dissociate? This Is the Mechanistic Question in C-H Hydroxylation by Heme and Nonheme Metal-Oxo Complexes. *Chem. Soc. Rev.* **2016**, *45*, 1197−1210.
(48) Groves, J. T.; Van der Puy, M. Stereospecific Aliphatic Hydroxylation by Iron-Hydrogen Peroxide. Evidence for a Stepwise Process. *J. Am. Chem. Soc.* **1976**, *98*, 5290−5297.
(49) Groves, J. T.; McClusky, G. A. Aliphatic Hydroxylation via Oxygen Rebound. Oxygen Transfer Catalyzed by Iron. *J. Am. Chem. Soc.* **1976**, *98*, 859−861.
(50) Wang, X.; Peter, S.; Kinne, M.; Hofrichter, M.; Groves, J. T. Detection and Kinetic Characterization of a Highly Reactive Heme−Thiolate Peroxygenase Compound I. *J. Am. Chem. Soc.* **2012**, *134*, 12897−12900.
(51) Yosca, T. H.; Rittle, J.; Krest, C. M.; Onderko, E. L.; Silakov, A.; Calixto, J. C.; Behan, R. K.; Green, M. T. Iron(IV)hydroxide p*Ka* and the Role of Thiolate Ligation in C−H Bond Activation by Cytochrome P450. *Science* **2013**, *342*, 825−829.
(52) Wang, X.; Ullrich, R.; Hofrichter, M.; Groves, J. T. Heme-Thiolate Ferryl of Aromatic Peroxygenase Is Basic and Reactive. *Proc. Natl. Acad. Sci. U. S. A.* **2015**, *112*, 3686−3691.
(53) Bordwell, F. G. Equilibrium Acidities in Dimethyl Sulfoxide Solution. *Acc. Chem. Res.* **1988**, *21*, 456−463.
(54) Fujii, H. Electronic Structure and Reactivity of High-Valent Oxo Iron Porphyrins. *Coord. Chem. Rev.* **2002**, *226*, 51−60.
(55) Dolphin, D.; Traylor, T. G.; Xie, L. Y. Polyhaloporphyrins: Unusual Ligands for Metals and Metal-Catalyzed Oxidations. *Acc. Chem. Res.* **1997**, *30*, 251−259.
(56) Costas, M. Selective C−H Oxidation Catalyzed by Metalloporphyrins. *Coord. Chem. Rev.* **2011**, *255*, 2912−2932.
(57) Watanabe, Y.; Nakajima, H.; Ueno, T. Reactivities of Oxo and Peroxo Intermediates Studied by Hemoprotein Mutants. *Acc. Chem. Res.* **2007**, *40*, 554−562.
(58) Huang, X.; Groves, J. T. Beyond Ferryl-Mediated Hydroxylation: 40 Years of the Rebound Mechanism and C−H Activation. *J. Biol. Inorg. Chem.* **2017**, *22*, 185−207.
(59) Schröder, D.; Shaik, S.; Schwarz, H. Two-State Reactivity as a New Concept in Organometallic Chemistry. *Acc. Chem. Res.* **2000**, *33*, 139−145.

DOI: 10.1021/acscentsci.8b00698
ACS Cent. Sci. 2019, 5, 13−28

(60) Shaik, S.; de Visser, S. P.; Ogliaro, F.; Schwarz, H.; Schröder, D. Two-State Reactivity Mechanisms of Hydroxylation and Epoxidation by Cytochrome P-450 Revealed by Theory. *Curr. Opin. Chem. Biol.* **2002**, *6*, 556−567.
(61) Shaik, S.; Kumar, D.; de Visser, S. P.; Altun, A.; Thiel, W. Theoretical Perspective on the Structure and Mechanism of Cytochrome P450 Enzymes. *Chem. Rev.* **2005**, *105*, 2279−2328.
(62) Jin, N.; Groves, J. T. Unusual Kinetic Stability of a Ground-State Singlet Oxomanganese(V) Porphyrin. Evidence for a Spin State Crossing Effect. *J. Am. Chem. Soc.* **1999**, *121*, 2923−2924.
(63) Jin, N.; Ibrahim, M.; Spiro, T. G.; Groves, J. T. Trans-dioxo Manganese(V) Porphyrins. *J. Am. Chem. Soc.* **2007**, *129*, 12416−12417.
(64) De Angelis, F.; Jin, N.; Car, R.; Groves, J. T. Electronic Structure and Reactivity of Isomeric Oxo-Mn(V) Porphyrins: Effects of Spin-State Crossing and p*K*a Modulation. *Inorg. Chem.* **2006**, *45*, 4268−4276.
(65) Takahashi, A.; Kurahashi, T.; Fujii, H. Redox Potentials of Oxoiron(IV) Porphyrin π-Cation Radical Complexes: Participation of Electron Transfer Process in Oxygenation Reactions. *Inorg. Chem.* **2011**, *50*, 6922−6928.
(66) Bell, S. R.; Groves, J. T. A Highly Reactive P450 Model Compound I. *J. Am. Chem. Soc.* **2009**, *131*, 9640−9641.
(67) Kang, Y.; Chen, H.; Jeong, Y. J.; Lai, W.; Bae, E. H.; Shaik, S.; Nam, W. Enhanced Reactivities of Iron(IV)-Oxo Porphyrin π-Cation Radicals in Oxygenation Reactions by Electron-Donating Axial Ligands. *Chem. - Eur. J.* **2009**, *15*, 10039−10046.
(68) Balcells, D.; Raynaud, C.; Crabtree, R. H.; Eisenstein, O. A Rational Basis for the Axial Ligand Effect in C−H Oxidation by $[MnO(porphyrin)(X)]^+$ (X = H_2O, OH^-, O^{2-}) from a DFT Study. *Inorg. Chem.* **2008**, *47*, 10090−10099.
(69) Takahashi, A.; Yamaki, D.; Ikemura, K.; Kurahashi, T.; Ogura, T.; Hada, M.; Fujii, H. Effect of the Axial Ligand on the Reactivity of the Oxoiron(IV) Porphyrin π-Cation Radical Complex: Higher Stabilization of the Product State Relative to the Reactant State. *Inorg. Chem.* **2012**, *51*, 7296−7305.
(70) Liu, W.; Cheng, M.-J.; Nielsen, R. J.; Goddard, W. A.; Groves, J. T. Probing the C−O Bond-Formation Step in Metalloporphyrin-Catalyzed C−H Oxygenation Reactions. *ACS Catal.* **2017**, *7*, 4182−4188.
(71) Groves, J. T.; Nemo, T. E.; Myers, R. S. Hydroxylation and Epoxidation Catalyzed by Iron-Porphine Complexes. Oxygen Transfer from Iodosylbenzene. *J. Am. Chem. Soc.* **1979**, *101*, 1032−1033.
(72) Gopalaiah, K. Chiral Iron Catalysts for Asymmetric Synthesis. *Chem. Rev.* **2013**, *113*, 3248−3296.
(73) Rose, E.; Andrioletti, B.; Zrig, S.; Quelquejeu-Ethève, M. Enantioselective Epoxidation of Olefins with Chiral Metalloporphyrin Catalysts. *Chem. Soc. Rev.* **2005**, *34*, 573−583.
(74) Meunier, B. Metalloporphyrins as Versatile Catalysts for Oxidation Reactions and Oxidative DNA Cleavage. *Chem. Rev.* **1992**, *92*, 1411−1456.
(75) Chang, C. K.; Kuo, M.-S. Reaction of Iron(III) Porphyrins and Iodosoxylene. The Active Oxene Complex of Cytochrome P-450. *J. Am. Chem. Soc.* **1979**, *101*, 3413−3415.
(76) Ellis, P. E.; Lyons, J. E. Selective Air Oxidation of Light Alkanes Catalyzed by Activated Metalloporphyrins - the Search for a Suprabiotic System. *Coord. Chem. Rev.* **1990**, *105*, 181−193.
(77) Li, G.; Dilger, A. K.; Cheng, P. T.; Ewing, W. R.; Groves, J. T. Selective C−H Halogenation with a Highly Fluorinated Manganese Porphyrin. *Angew. Chem., Int. Ed.* **2018**, *57*, 1251−1255.
(78) Huang, X.; Zhuang, T.; Kates, P. A.; Gao, H.; Chen, X.; Groves, J. T. Alkyl Isocyanates via Manganese-Catalyzed C−H Activation for the Preparation of Substituted Ureas. *J. Am. Chem. Soc.* **2017**, *139*, 15407−15413.
(79) Krebs, C.; Galonić Fujimori, D.; Walsh, C. T.; Bollinger, J. M., Jr. Non-Heme Fe(IV)−Oxo Intermediates. *Acc. Chem. Res.* **2007**, *40*, 484−492.
(80) Price, J. C.; Barr, E. W.; Tirupati, B.; Bollinger, J. M., Jr.; Krebs, C. The First Direct Characterization of a High-Valent Iron Intermediate in the Reaction of an α-Ketoglutarate-Dependent Dioxygenase: A High-Spin Fe(IV) Complex in Taurine/α-Ketoglutarate Dioxygenase (TauD) from *Escherichia coli*. *Biochemistry* **2003**, *42*, 7497−7508.
(81) Proshlyakov, D. A.; Henshaw, T. F.; Monterosso, G. R.; Ryle, M. J.; Hausinger, R. P. Direct Detection of Oxygen Intermediates in the Non-Heme Fe Enzyme Taurine/α-Ketoglutarate Dioxygenase. *J. Am. Chem. Soc.* **2004**, *126*, 1022−1023.
(82) Riggs-Gelasco, P. J.; Price, J. C.; Guyer, R. B.; Brehm, J. H.; Barr, E. W.; Bollinger, J. M., Jr.; Krebs, C. EXAFS Spectroscopic Evidence for an Fe = O Unit in the Fe(IV) Intermediate Observed during Oxygen Activation by Taurine:α-Ketoglutarate Dioxygenase. *J. Am. Chem. Soc.* **2004**, *126*, 8108−8109.
(83) Wong, S. D.; Srnec, M.; Matthews, M. L.; Liu, L. V.; Kwak, Y.; Park, K.; Bell, C. B., III; Alp, E. E.; Zhao, J.; Yoda, Y.; Kitao, S.; Seto, M.; Krebs, C.; Bollinger, J. M., Jr.; Solomon, E. I. Elucidation of the Fe(IV)═O Intermediate in the Catalytic Cycle of the Halogenase SyrB2. *Nature* **2013**, *499*, 320−323.
(84) Price, J. C.; Barr, E. W.; Glass, T. E.; Krebs, C.; Bollinger, J. M., Jr. Evidence for Hydrogen Abstraction from C1 of Taurine by the High-Spin Fe(IV) Intermediate Detected during Oxygen Activation by Taurine:α-Ketoglutarate Dioxygenase (TauD). *J. Am. Chem. Soc.* **2003**, *125*, 13008−13009.
(85) Panay, A. J.; Fitzpatrick, P. F. Kinetic Isotope Effects on Aromatic and Benzylic Hydroxylation by *Chromobacterium violaceum* Phenylalanine Hydroxylase as Probes of Chemical Mechanism and Reactivity. *Biochemistry* **2008**, *47*, 11118−11124.
(86) Panay, A. J.; Lee, M.; Krebs, C.; Bollinger, J. M., Jr.; Fitzpatrick, P. F. Evidence for a High-Spin Fe(IV) Species in the Catalytic Cycle of a Bacterial Phenylalanine Hydroxylase. *Biochemistry* **2011**, *50*, 1928−1933.
(87) Eser, B. E.; Barr, E. W.; Frantom, P. A.; Saleh, L.; Bollinger, J. M., Jr.; Krebs, C.; Fitzpatrick, P. F. Direct Spectroscopic Evidence for a High-Spin Fe(IV) Intermediate in Tyrosine Hydroxylase. *J. Am. Chem. Soc.* **2007**, *129*, 11334−11335.
(88) Frantom, P. A.; Pongdee, R.; Sulikowski, G. A.; Fitzpatrick, P. F. Intrinsic Deuterium Isotope Effects on Benzylic Hydroxylation by Tyrosine Hydroxylase. *J. Am. Chem. Soc.* **2002**, *124*, 4202−4203.
(89) Miller, R. J.; Benkovic, S. J. L-[2,5-H_2]Phenylalanine, an Alternate Substrate for Rat Liver Phenylalanine Hydroxylase. *Biochemistry* **1988**, *27*, 3658−3663.
(90) Yan, W.; Song, H.; Song, F.; Guo, Y.; Wu, C.-H.; Sae Her, A.; Pu, Y.; Wang, S.; Naowarojna, N.; Weitz, A.; Hendrich, M. P.; Costello, C. E.; Zhang, L.; Liu, P.; Jessie Zhang, Y. Endoperoxide Formation by an α-Ketoglutarate-Dependent Mononuclear Non-Haem Iron Enzyme. *Nature* **2015**, *527*, 539−543.
(91) Grapperhaus, C. A.; Mienert, B.; Bill, E.; Weyhermüller, T.; Wieghardt, K. Mononuclear (Nitrido)iron(V) and (Oxo)iron(IV) Complexes via Photolysis of $[(cyclam\text{-}acetato)Fe^{III}(N_3)]^+$ and Ozonolysis of $[(cyclam\text{-}acetato)Fe^{III}(O_3SCF_3)]^+$ in Water/Acetone Mixtures. *Inorg. Chem.* **2000**, *39*, 5306−5317.
(92) Nam, W.; Lee, Y.-M.; Fukuzumi, S. Tuning Reactivity and Mechanism in Oxidation Reactions by Mononuclear Nonheme Iron(IV)-Oxo Complexes. *Acc. Chem. Res.* **2014**, *47*, 1146−1154.
(93) Usharani, D.; Janardanan, D.; Li, C.; Shaik, S. A Theory for Bioinorganic Chemical Reactivity of Oxometal Complexes and Analogous Oxidants: The Exchange and Orbital-Selection Rules. *Acc. Chem. Res.* **2013**, *46*, 471−482.
(94) McDonald, A. R.; Que, L., Jr. High-Valent Nonheme Iron-Oxo Complexes: Synthesis, Structure, and Spectroscopy. *Coord. Chem. Rev.* **2013**, *257*, 414−428.
(95) Hohenberger, J.; Ray, K.; Meyer, K. The Biology and Chemistry of High-Valent Iron−Oxo and Iron−Nitrido Complexes. *Nat. Commun.* **2012**, *3*, 720−732.
(96) Shaik, S.; Chen, H.; Janardanan, D. Exchange-Enhanced Reactivity in Bond Activation by Metal−Oxo Enzymes and Synthetic Reagents. *Nat. Chem.* **2011**, *3*, 19−27.
(97) Hirao, H.; Que, L., Jr.; Nam, W.; Shaik, S. A Two-State Reactivity Rationale for Counterintuitive Axial Ligand Effects on the

DOI: 10.1021/acscentsci.8b00698
ACS Cent. Sci. 2019, 5, 13−28

C-H Activation Reactivity of Nonheme Fe^{IV}=O Oxidants. *Chem. - Eur. J.* **2008**, *14*, 1740−1756.
(98) Sastri, C. V.; Lee, J.; Oh, K.; Lee, Y. J.; Lee, J.; Jackson, T. A.; Ray, K.; Hirao, H.; Shin, W.; Halfen, J. A.; Kim, J.; Que, L., Jr.; Shaik, S.; Nam, W. Axial Ligand Tuning of a Nonheme Iron(IV)−Oxo Unit for Hydrogen Atom Abstraction. *Proc. Natl. Acad. Sci. U. S. A.* **2007**, *104*, 19181−19186.
(99) Sahu, S.; Zhang, B.; Pollock, C. J.; Dürr, M.; Davies, C. G.; Confer, A. M.; Ivanović-Burmazović, I.; Siegler, M. A.; Jameson, G. N. L.; Krebs, C.; Goldberg, D. P. Aromatic C−F Hydroxylation by Nonheme Iron(IV)−Oxo Complexes: Structural, Spectroscopic, and Mechanistic Investigations. *J. Am. Chem. Soc.* **2016**, *138*, 12791−12802.
(100) Sahu, S.; Quesne, M. G.; Davies, C. G.; Dürr, M.; Ivanović-Burmazović, I.; Siegler, M. A.; Jameson, G. N. L.; de Visser, S. P.; Goldberg, D. P. Direct Observation of a Nonheme Iron(IV)−Oxo Complex That Mediates Aromatic C−F Hydroxylation. *J. Am. Chem. Soc.* **2014**, *136*, 13542−13545.
(101) Ye, S.; Neese, F. Nonheme Oxo-Iron(IV) Intermediates Form an Oxyl Radical upon Approaching the C−H Bond Activation Transition State. *Proc. Natl. Acad. Sci. U. S. A.* **2011**, *108*, 1228−1233.
(102) Shaik, S.; Hirao, H.; Kumar, D. Reactivity of High-Valent Iron−Oxo Species in Enzymes and Synthetic Reagents: A Tale of Many States. *Acc. Chem. Res.* **2007**, *40*, 532−542.
(103) Biswas, A. N.; Puri, M.; Meier, K. K.; Oloo, W. N.; Rohde, G. T.; Bominaar, E. L.; Münck, E.; Que, L., Jr. Modeling TauD-J: A High-Spin Nonheme Oxoiron(IV) Complex with High Reactivity toward C-H Bonds. *J. Am. Chem. Soc.* **2015**, *137*, 2428−2431.
(104) Seo, M. S.; Kim, N. H.; Cho, K.-B.; So, J. E.; Park, S. K.; Clemancey, M.; Garcia-Serres, R.; Latour, J.-M.; Shaik, S.; Nam, W. A Mononuclear Nonheme Iron(IV)-Oxo Complex Which Is More Reactive Than Cytochrome P450 Model Compound I. *Chem. Sci.* **2011**, *2*, 1039−1045.
(105) Monte-Pérez, I.; Engelmann, X.; Lee, Y.-M.; Yoo, M.; Kumaran, E.; Farquhar, E. R.; Bill, E.; England, J.; Nam, W.; Swart, M.; Ray, K. A Highly Reactive Oxoiron(IV) Complex Supported by a Bioinspired N_3O Macrocyclic Ligand. *Angew. Chem., Int. Ed.* **2017**, *56*, 14384−14388.
(106) Kupper, C.; Mondal, B.; Serrano-Plana, J.; Klawitter, I.; Neese, F.; Costas, M.; Ye, S.; Meyer, F. Nonclassical Single-State Reactivity of an Oxo-Iron(IV) Complex Confined to Triplet Pathways. *J. Am. Chem. Soc.* **2017**, *139*, 8939−8949.
(107) Ye, S.; Kupper, C.; Meyer, S.; Andris, E.; Navrátil, R.; Krahe, O.; Mondal, B.; Atanasov, M.; Bill, E.; Roithová, J.; Meyer, F.; Neese, F. Magnetic Circular Dichroism Evidence for an Unusual Electronic Structure of a Tetracarbene−Oxoiron(IV) Complex. *J. Am. Chem. Soc.* **2016**, *138*, 14312−14325.
(108) Meyer, S.; Klawitter, I.; Demeshko, S.; Bill, E.; Meyer, F. A Tetracarbene−Oxoiron(IV) Complex. *Angew. Chem., Int. Ed.* **2013**, *52*, 901−905.
(109) Ansari, A.; Kaushik, A.; Rajaraman, G. Mechanistic Insights on the *ortho*-Hydroxylation of Aromatic Compounds by Non-heme Iron Complex: A Computational Case Study on the Comparative Oxidative Ability of Ferric-Hydroperoxo and High-Valent Fe^{IV}=O and Fe^{V}=O Intermediates. *J. Am. Chem. Soc.* **2013**, *135*, 4235−4249.
(110) Srnec, M.; Wong, S. D.; England, J.; Que, L., Jr.; Solomon, E. I. π-Frontier Molecular Orbitals in S = 2 Ferryl Species and Elucidation of Their Contributions to Reactivity. *Proc. Natl. Acad. Sci. U. S. A.* **2012**, *109*, 14326−14331.
(111) McDonald, A. R.; Guo, Y.; Vu, V. V.; Bominaar, E. L.; Münck, E.; Que, L., Jr. A Mononuclear Carboxylate-Rich Oxoiron(IV) Complex: A Structural and Functional Mimic of TauD Intermediate 'J'. *Chem. Sci.* **2012**, *3*, 1680−1693.
(112) de Visser, S. P.; Oh, K.; Han, A.-R.; Nam, W. Combined Experimental and Theoretical Study on Aromatic Hydroxylation by Mononuclear Nonheme Iron(IV)−Oxo Complexes. *Inorg. Chem.* **2007**, *46*, 4632−4641.
(113) Sahu, S.; Widger, L. R.; Quesne, M. G.; de Visser, S. P.; Matsumura, H.; Moënne-Loccoz, P.; Siegler, M. A.; Goldberg, D. P. Secondary Coordination Sphere Influence on the Reactivity of Nonheme Iron(II) Complexes: An Experimental and DFT Approach. *J. Am. Chem. Soc.* **2013**, *135*, 10590−10593.
(114) Fukuzumi, S.; Kotani, H.; Suenobu, T.; Hong, S.; Lee, Y.-M.; Nam, W. Contrasting Effects of Axial Ligands on Electron-Transfer Versus Proton-Coupled Electron-Transfer Reactions of Nonheme Oxoiron(IV) Complexes. *Chem. - Eur. J.* **2010**, *16*, 354−361.
(115) Jackson, T. A.; Rohde, J.-U.; Seo, M. S.; Sastri, C. V.; DeHont, R.; Stubna, A.; Ohta, T.; Kitagawa, T.; Münck, E.; Nam, W.; Que, L., Jr. Axial Ligand Effects on the Geometric and Electronic Structures of Nonheme Oxoiron(IV) Complexes. *J. Am. Chem. Soc.* **2008**, *130*, 12394−12407.
(116) Mandal, D.; Ramanan, R.; Usharani, D.; Janardanan, D.; Wang, B.; Shaik, S. How Does Tunneling Contribute to Counter-intuitive H-Abstraction Reactivity of Nonheme Fe(IV)O Oxidants with Alkanes? *J. Am. Chem. Soc.* **2015**, *137*, 722−733.
(117) Fukuzumi, S.; Morimoto, Y.; Kotani, H.; Naumov, P.; Lee, Y.-M.; Nam, W. Crystal Structure of a Metal Ion-Bound Oxoiron(IV) Complex and Implications for Biological Electron Transfer. *Nat. Chem.* **2010**, *2*, 756−759.
(118) Morimoto, Y.; Kotani, H.; Park, J.; Lee, Y.-M.; Nam, W.; Fukuzumi, S. Metal Ion-Coupled Electron Transfer of a Nonheme Oxoiron(IV) Complex: Remarkable Enhancement of Electron-Transfer Rates by Sc^{3+}. *J. Am. Chem. Soc.* **2011**, *133*, 403−405.
(119) Park, J.; Morimoto, Y.; Lee, Y.-M.; Nam, W.; Fukuzumi, S. Proton-Promoted Oxygen Atom Transfer vs Proton-Coupled Electron Transfer of a Non-Heme Iron(IV)-Oxo Complex. *J. Am. Chem. Soc.* **2012**, *134*, 3903−3911.
(120) Young, K. J.; Brennan, B. J.; Tagore, R.; Brudvig, G. W. Photosynthetic Water Oxidation: Insights from Manganese Model Chemistry. *Acc. Chem. Res.* **2015**, *48*, 567−574.
(121) Yano, J.; Yachandra, V. Mn_4Ca Cluster in Photosynthesis: Where and How Water is Oxidized to Dioxygen. *Chem. Rev.* **2014**, *114*, 4175−4205.
(122) Cox, N.; Pantazis, D. A.; Neese, F.; Lubitz, W. Biological Water Oxidation. *Acc. Chem. Res.* **2013**, *46*, 1588−1596.
(123) Nocera, D. G. The Artificial Leaf. *Acc. Chem. Res.* **2012**, *45*, 767−776.
(124) Bryliakov, K. P. Catalytic Asymmetric Oxygenations with the Environmentally Benign Oxidants H_2O_2 and O_2. *Chem. Rev.* **2017**, *117*, 11406−11459.
(125) Wu, X.; Seo, M. S.; Davis, K. M.; Lee, Y.-M.; Chen, J.; Cho, K.-B.; Pushkar, Y. N.; Nam, W. A Highly Reactive Mononuclear Non-Heme Manganese(IV)−Oxo Complex That Can Activate the Strong C−H Bonds of Alkanes. *J. Am. Chem. Soc.* **2011**, *133*, 20088−20091.
(126) Cho, K.-B.; Shaik, S.; Nam, W. Theoretical Investigations into C−H Bond Activation Reaction by Nonheme $Mn^{IV}O$ Complexes: Multistate Reactivity with No Oxygen Rebound. *J. Phys. Chem. Lett.* **2012**, *3*, 2851−2856.
(127) Chen, J.; Lee, Y.-M.; Davis, K. M.; Wu, X.; Seo, M. S.; Cho, K.-B.; Yoon, H.; Park, Y. J.; Fukuzumi, S.; Pushkar, Y. N.; Nam, W. A Mononuclear Non-Heme Manganese(IV)−Oxo Complex Binding Redox-Inactive Metal Ions. *J. Am. Chem. Soc.* **2013**, *135*, 6388−6391.
(128) Leto, D. F.; Ingram, R.; Day, V. W.; Jackson, T. A. Spectroscopic Properties and Reactivity of a Mononuclear Oxomanganese(IV) Complex. *Chem. Commun.* **2013**, *49*, 5378−5380.
(129) Chen, J.; Yoon, H.; Lee, Y.-M.; Seo, M. S.; Sarangi, R.; Fukuzumi, S.; Nam, W. Tuning the Reactivity of Mononuclear Nonheme Manganese(IV)-Oxo Complexes by Triflic Acid. *Chem. Sci.* **2015**, *6*, 3624−3632.
(130) Barman, P.; Vardhaman, A. K.; Martin, B.; Wörner, S. J.; Sastri, C. V.; Comba, P. Influence of Ligand Architecture on Oxidation Reactions by High-Valent Nonheme Manganese Oxo Complexes Using Water as a Source of Oxygen. *Angew. Chem., Int. Ed.* **2015**, *54*, 2095−2099.
(131) Kim, S.; Cho, K.-B.; Lee, Y.-M.; Chen, J.; Fukuzumi, S.; Nam, W. Factors Controlling the Chemoselectivity in the Oxidation of Olefins by Nonheme Manganese(IV)-Oxo Complexes. *J. Am. Chem. Soc.* **2016**, *138*, 10654−10663.

DOI: 10.1021/acscentsci.8b00698
ACS Cent. Sci. 2019, 5, 13−28

(132) Xiao, D. J.; Bloch, E. D.; Mason, J. A.; Queen, W. L.; Hudson, M. R.; Planas, N.; Borycz, J.; Dzubak, A. L.; Verma, P.; Lee, K.; Bonino, F.; Crocellà, V.; Yano, J.; Bordiga, S.; Truhlar, D. G.; Gagliardi, L.; Brown, C. M.; Long, J. R. Oxidation of Ethane to Ethanol by N_2O in a Metal−Organic Framework with Coordinatively Unsaturated Iron(II) Sites. *Nat. Chem.* **2014**, *6*, 590−595.
(133) Verma, P.; Vogiatzis, K. D.; Planas, N.; Borycz, J.; Xiao, D. J.; Long, J. R.; Gagliardi, L.; Truhlar, D. G. Mechanism of Oxidation of Ethane to Ethanol at Iron(IV)−Oxo Sites in Magnesium-Diluted Fe_2(dobdc). *J. Am. Chem. Soc.* **2015**, *137*, 5770−5781.
(134) Que, L., Jr.; Tolman, W. B. Biologically Inspired Oxidation Catalysis. *Nature* **2008**, *455*, 333−340.
(135) Karlsson, A.; Parales, J. V.; Parales, R. E.; Gibson, D. T.; Eklund, H.; Ramaswamy, S. Crystal Structure of Naphthalene Dioxygenase: Side-on Binding of Dioxygen to Iron. *Science* **2003**, *299*, 1039−1042.
(136) Neibergall, M. B.; Stubna, A.; Mekmouche, Y.; Münck, E.; Lipscomb, J. D. Hydrogen Peroxide Dependent *cis*-Dihydroxylation of Benzoate by Fully Oxidized Benzoate 1,2-Dioxygenase. *Biochemistry* **2007**, *46*, 8004−8016.
(137) Olivo, G.; Cussó, O.; Costas, M. Biologically Inspired C−H and C = C Oxidations with Hydrogen Peroxide Catalyzed by Iron Coordination Complexes. *Chem. - Asian J.* **2016**, *11*, 3148−3158.
(138) Prat, I.; Mathieson, J. S.; Güell, M.; Ribas, X.; Luis, J. M.; Cronin, L.; Costas, M. Observation of Fe(V)═O Using Variable-Temperature Mass Spectrometry and Its Enzyme-like C−H and C = C Oxidation Reactions. *Nat. Chem.* **2011**, *3*, 788−793.
(139) Chen, M. S.; White, M. C. A Predictably Selective Aliphatic C−H Oxidation Reaction for Complex Molecule Synthesis. *Science* **2007**, *318*, 783−787.
(140) Olivo, G.; Cussó, O.; Borrell, M.; Costas, M. Oxidation of Alkane and Alkene Moieties with Biologically Inspired Nonheme Iron Catalysts and Hydrogen Peroxide: from Free Radicals to Stereoselective Transformations. *J. Biol. Inorg. Chem.* **2017**, *22*, 425−452.
(141) Lyakin, O. Y.; Zima, A. M.; Samsonenko, D. G.; Bryliakov, K. P.; Talsi, E. P. EPR Spectroscopic Detection of the Elusive Fe^{V}=O Intermediates in Selective Catalytic Oxofunctionalizations of Hydrocarbons Mediated by Biomimetic Ferric Complexes. *ACS Catal.* **2015**, *5*, 2702−2707.
(142) Oloo, W. N.; Meier, K. K.; Wang, Y.; Shaik, S.; Münck, E.; Que, L., Jr. Identification of a Low-Spin Acylperoxoiron(III) Intermediate in Bio-Inspired Non-Heme Iron-Catalysed Oxidations. *Nat. Commun.* **2014**, *5*, 3046−3054.
(143) Wu, M.; Miao, C.-X.; Wang, S.; Hu, X.; Xia, C.; Kühn, F. E.; Sun, W. Chiral Bioinspired Non-Heme Iron Complexes for Enantioselective Epoxidation of α,β-Unsaturated Ketones. *Adv. Synth. Catal.* **2011**, *353*, 3014−3022.
(144) Feng, Y.; England, J.; Que, L., Jr. Iron-Catalyzed Olefin Epoxidation and cis-Dihydroxylation by Tetraalkylcyclam Complexes: the Importance of cis-Labile Sites. *ACS Catal.* **2011**, *1*, 1035−1042.
(145) Serrano-Plana, J.; Oloo, W. N.; Acosta-Rueda, L.; Meier, K. K.; Verdejo, B.; García-España, E.; Basallote, M. G.; Münck, E.; Que, L., Jr.; Company, A.; Costas, M. Trapping a Highly Reactive Nonheme Iron Intermediate That Oxygenates Strong C—H Bonds with Stereoretention. *J. Am. Chem. Soc.* **2015**, *137*, 15833−15842.
(146) Ghosh, M.; Singh, K. K.; Panda, C.; Weitz, A.; Hendrich, M. P.; Collins, T. J.; Dhar, B. B.; Sen Gupta, S. Formation of a Room Temperature Stable Fe^{V}(O) Complex: Reactivity Toward Unactivated C−H Bonds. *J. Am. Chem. Soc.* **2014**, *136*, 9524−9527.
(147) Du, J.; Miao, C.; Xia, C.; Lee, Y.-M.; Nam, W.; Sun, W. Mechanistic Insights into the Enantioselective Epoxidation of Olefins by Bioinspired Manganese Complexes: Role of Carboxylic Acid and Nature of Active Oxidant. *ACS Catal.* **2018**, *8*, 4528−4538.
(148) Milan, M.; Bietti, M.; Costas, M. Highly Enantioselective Oxidation of Nonactivated Aliphatic C−H Bonds with Hydrogen Peroxide Catalyzed by Manganese Complexes. *ACS Cent. Sci.* **2017**, *3*, 196−204.
(149) Miao, C.; Wang, B.; Wang, Y.; Xia, C.; Lee, Y.-M.; Nam, W.; Sun, W. Proton-Promoted and Anion-Enhanced Epoxidation of Olefins by Hydrogen Peroxide in the Presence of Nonheme Manganese Catalysts. *J. Am. Chem. Soc.* **2016**, *138*, 936−943.
(150) Bryliakov, K. P.; Talsi, E. P. Active Sites and Mechanisms of Bioinspired Oxidation with H_2O_2, Catalyzed by Non-Heme Fe and Related Mn Complexes. *Coord. Chem. Rev.* **2014**, *276*, 73−96.
(151) Saisaha, P.; de Boer, J. W.; Browne, W. R. Mechanisms in Manganese Catalysed Oxidation of Alkenes with H_2O_2. *Chem. Soc. Rev.* **2013**, *42*, 2059−2074.
(152) Talsi, E. P.; Bryliakov, K. P. Chemo- and Stereoselective C-H Oxidations and Epoxidations/cis-Dihydroxylations with H_2O_2, Catalyzed by Non-Heme Iron and Manganese Complexes. *Coord. Chem. Rev.* **2012**, *256*, 1418−1434.
(153) Cook, S. A.; Borovik, A. S. Molecular Designs for Controlling the Local Environments around Metal Ions. *Acc. Chem. Res.* **2015**, *48*, 2407−2414.
(154) Marshall, N. M.; Garner, D. K.; Wilson, T. D.; Gao, Y.-G.; Robinson, H.; Nilges, M. J.; Lu, Y. Rationally Tuning the Reduction Potential of A Single Cupredoxin Beyond the Natural Range. *Nature* **2009**, *462*, 113.
(155) Matson, E. M.; Park, Y. J.; Fout, A. R. Facile Nitrite Reduction in a Non-heme Iron System: Formation of an Iron(III)-Oxo. *J. Am. Chem. Soc.* **2014**, *136*, 17398−17401.
(156) MacBeth, C. E.; Golombek, A. P.; Young, V. G.; Yang, C.; Kuczera, K.; Hendrich, M. P.; Borovik, A. S. O_2 Activation by Nonheme Iron Complexes: A Monomeric Fe(III)-Oxo Complex Derived From O_2. *Science* **2000**, *289*, 938−941.
(157) Rigsby, M. L.; Wasylenko, D. J.; Pegis, M. L.; Mayer, J. M. Medium Effects Are as Important as Catalyst Design for Selectivity in Electrocatalytic Oxygen Reduction by Iron−Porphyrin Complexes. *J. Am. Chem. Soc.* **2015**, *137*, 4296−4299.
(158) Matson, B. D.; Carver, C. T.; Von Ruden, A.; Yang, J. Y.; Raugei, S.; Mayer, J. M. Distant Protonated Pyridine Groups in Water-Soluble Iron Porphyrin Electrocatalysts Promote Selective Oxygen Reduction to Water. *Chem. Commun.* **2012**, *48*, 11100−11102.
(159) Carver, C. T.; Matson, B. D.; Mayer, J. M. Electrocatalytic Oxygen Reduction by Iron Tetra-arylporphyrins Bearing Pendant Proton Relays. *J. Am. Chem. Soc.* **2012**, *134*, 5444−5447.
(160) Shook, R. L.; Peterson, S. M.; Greaves, J.; Moore, C.; Rheingold, A. L.; Borovik, A. S. Catalytic Reduction of Dioxygen to Water with a Monomeric Manganese Complex at Room Temperature. *J. Am. Chem. Soc.* **2011**, *133*, 5810−5817.
(161) Shook, R. L.; Gunderson, W. A.; Greaves, J.; Ziller, J. W.; Hendrich, M. P.; Borovik, A. S. A Monomeric Mn^{III}−Peroxo Complex Derived Directly from Dioxygen. *J. Am. Chem. Soc.* **2008**, *130*, 8888−8889.
(162) Kal, S.; Draksharapu, A.; Que, L., Jr. Sc^{3+} (or $HClO_4$) Activation of a Nonheme Fe^{III}−OOH Intermediate for the Rapid Hydroxylation of Cyclohexane and Benzene. *J. Am. Chem. Soc.* **2018**, *140*, 5798−5804.
(163) Du, H.; Lo, P.-K.; Hu, Z.; Liang, H.; Lau, K.-C.; Wang, Y.-N.; Lam, W. W. Y.; Lau, T.-C. Lewis Acid-Activated Oxidation of Alcohols by Permanganate. *Chem. Commun.* **2011**, *47*, 7143−7145.
(164) Lam, W. W. Y.; Yiu, S.-M.; Lee, J. M. N.; Yau, S. K. Y.; Kwong, H.-K.; Lau, T.-C.; Liu, D.; Lin, Z. BF_3-Activated Oxidation of Alkanes by MnO_4. *J. Am. Chem. Soc.* **2006**, *128*, 2851−2858.
(165) Kolb, H. C.; VanNieuwenhze, M. S.; Sharpless, K. B. Catalytic Asymmetric Dihydroxylation. *Chem. Rev.* **1994**, *94*, 2483−2547.
(166) Chatterjee, S.; Paine, T. K. Olefin *cis*-Dihydroxylation and Aliphatic C-H Bond Oxygenation by a Dioxygen-Derived Electrophilic Iron-Oxygen Oxidant. *Angew. Chem., Int. Ed.* **2015**, *54*, 9338−9342.

DOI: 10.1021/acscentsci.8b00698
ACS Cent. Sci. 2019, 5, 13−28